

THESIS

EVALUATING HABITAT SUITABILITY AND CONNECTIVITY FOR THE ENDANGERED  
NORTHERNMOST POPULATION OF JAGUARS (*PANTHERA ONCA*)

Submitted by

Vincent A. Landau

Graduate Degree Program in Ecology

In partial fulfillment of the requirements

For the Degree of Master of Science

Colorado State University

Fort Collins, Colorado

Spring 2020

Master's Committee:

Advisor: Dr. Barry R. Noon

Co-Advisor: Dr. David M. Theobald

Dr. N. Thompson Hobbs

Copyright by Vincent A. Landau 2020

All Rights Reserved

## ABSTRACT

### EVALUATING HABITAT SUITABILITY AND CONNECTIVITY FOR THE ENDANGERED NORTHERNMOST POPULATION OF JAGUARS (*PANTHERA ONCA*)

Understanding the distribution of wildlife habitat as well as landscape connectivity for threatened or endangered wildlife populations provides valuable information for conservation planning efforts. The northernmost population of jaguars (*Panthera onca*) is threatened with extinction, and has been extirpated from much of its historic range in the United States due to habitat loss/fragmentation, hunting, and poaching. Recent efforts by the United States government to expand U.S.-Mexico border infrastructure threaten to further fragment jaguar habitat in the borderlands. Models of habitat for jaguars in the United States have been developed, but they can be improved by using a finer analytical resolution, appropriately accommodating uncertainty by using a statistical framework, and using more appropriate data. Existing connectivity models have also been at coarse resolution, been broad in scope, and have not explicitly considered to effects of U.S.-Mexico border infrastructure.

The Draft Recovery Plan for the jaguar was released by the United States Fish and Wildlife Service in 2017 and identified a need for additional research on jaguar habitat use and to identify key habitat and movement corridors in the U.S.-Mexico borderlands. To address these research needs, the goal of my thesis research was to provide updated and improved models of habitat and landscape connectivity for the northern population of jaguars in Sonora and Chihuahua, Mexico and Arizona and New Mexico, United States.

For Chapter one, I developed a novel statistical model and applied it to predict and explain habitat selection by the northern population of jaguars. The study area for this chapter encompassed the Madrean Sky Islands (a complex of small mountain ranges in southeastern Arizona, southwestern New Mexico, and northwestern Mexico) and surrounding areas. Like many imperiled species and

populations, data on jaguars are sparse, which limits our ability to gain insight into their ecology. To maximize inference, I developed a novel integrated Bayesian model that makes use of both presence-only and detection/non-detection data to model habitat selection. Results show that terrain ruggedness (+) and distance to riparian vegetation (-) are key predictors of habitat selection. There is a mean predicted 25,463 km<sup>2</sup> of jaguar habitat in the study area. A mean predicted 40.6% of this habitat lies in the United States, suggesting that habitat in the U.S. could play an important role in the long term persistence of the northern jaguar population if jaguars are able to recolonize the region.

In Chapter two, I turn focus to evaluating landscape connectivity, particularly in the context of U.S.-Mexico border infrastructure. I modeled landscape connectivity using Circuitscape, where the resistance surface was derived from the habitat suitability model from Chapter one in combination with human land use intensity and data on functional movement barriers (roads and border infrastructure). I evaluated the impacts of present-day border infrastructure as well as a likely future border scenario by running models for three different border infrastructure scenarios: 1) A scenario with no border infrastructure in place, 2) the present day border infrastructure scenario, and 3) a possible future scenario in which present day vehicle barriers are converted to pedestrian fencing. The resulting connectivity maps revealed that existing border infrastructure has far reaching consequences for habitat connectivity in the borderlands, and border wall expansion threatens to further isolate jaguar habitat in the United States from the breeding population in Mexico.

## ACKNOWLEDGEMENTS

My graduate education and this research was made possible through funding from Conservation Science Partners, Inc. (CSP) and the Wilburforce Foundation. I would like to thank them for their incredibly generous support. The camera trapping portion of this project was funded by Southern Illinois University, National Science Foundation Graduate Research Fellowship Program, Panthera, Shared Earth Foundation and Disney Wildlife Conservation Fund. We thank the ranchers who allowed us access onto their lands. S. Borrego and M. Galaz-Galaz collected data in the field. M. Culver, L. Haynes, J. Kolowski, C. López González, O. Rosas-Rosas, and R. Thompson provided additional logistical support.

Beyond funding for graduate school, CSP has provided me with professional experience, new skills, knowledge, and great memories over the past four-and-a-half years. I started working for CSP part time in 2015 after receiving my undergraduate degree. Shortly after, I transitioned to a full time position. Brett Dickson, President and Chief Scientist of CSP, saw potential in me and secured the funding to support my master's program. I cannot thank him enough. I would also like to thank the entire CSP staff for the great memories and for everything I have learned through working with them so far. I am happy to be working for CSP once again now that my graduate research is complete!

I would like to thank my advisor, Dr. Barry Noon, whose relentless pursuit of science and knowledge is only surpassed by his passion for nature and conservation. He has been an inspiration. My co-advisor, Dr. David Theobald's creativity, big picture thinking, and positive attitude has brought valuable perspective and enjoyment to my graduate research. Dr. Tom Hobbs, my committee member, has taught me incredibly valuable skills and has brought a spirit of scholarship and scientific rigor to my graduate research and education. All three of my committee members have been wonderful mentors, and I feel incredibly fortunate to have received their guidance. It has been a pleasure working with them.

Many others also helped make this research possible, more productive, and more enjoyable. Dr. Clay Nielsen's shared jaguar occupancy data with me for use in my research, which vastly improved my first chapter. Those data were critical to its quality and novelty. My research did not have a field component, but in 2018, Sergio Avila led a tour of the Arizona borderlands as part of the Biodiversity and Management of the Madrean Archipelago conference and provided insight into jaguar ecology and the ecological impacts of the border wall. I want to thank him and conference organizers for giving me valuable firsthand insight into my study system and species.

Finally I would like to thank the faculty, staff, and graduate students in the Department of Fish, Wildlife, and Conservation Biology and the Graduate Degree Program in Ecology. My fellow Noon lab students in particular, Rekha Warriar, Pranav Chanchani, Jess Shyvers, and Valerie Steen have been wonderful friends and colleagues. My experiences with them are the ones I'll look back on most fondly when thinking about graduate school.

On the non-academic side of things, my parents, Paul and Orissa, and my sisters Alex and Lydia have been great sources of support and encouragement. My friends, Mitch and Warren in particular, provided the often needed recharge and break from the stresses of grad school. Thank you all for everything.

## DEDICATION

*I dedicate this work to my grandfather, Vincent R. Landau.*

## TABLE OF CONTENTS

ABSTRACT . . . . .	ii
ACKNOWLEDGEMENTS . . . . .	iv
DEDICATION . . . . .	vi
LIST OF TABLES . . . . .	ix
LIST OF FIGURES . . . . .	x
Chapter 1	Integrating Presence-only and Occupancy Data to Model Habitat Selection for the Northernmost Population of Jaguars ( <i>Panthera onca</i> ) . . . . . 1
1.1	Introduction . . . . . 1
1.2	Methods . . . . . 4
1.2.1	Study Area . . . . . 4
1.2.2	Data . . . . . 4
1.2.3	Integrated Species Distribution Model . . . . . 6
1.2.4	Landscape Covariates . . . . . 9
1.2.5	Model Fitting . . . . . 12
1.2.6	Model Selection . . . . . 12
1.2.7	Model Validation . . . . . 13
1.2.8	Mapping and Analysis of Habitat . . . . . 14
1.3	Results . . . . . 15
1.4	Discussion . . . . . 16
1.4.1	Habitat Modeling . . . . . 16
1.4.2	Potential Conservation Implications . . . . . 19
1.4.3	Integrated Species Distribution Model . . . . . 20
1.4.4	Conclusions . . . . . 20
Chapter 2	Trans-border Connectivity Models for Jaguars ( <i>Panthera onca</i> ) Reveal US- Mexico Border Wall Impacts . . . . . 22
2.1	Introduction . . . . . 22
2.2	Methods . . . . . 25
2.2.1	Study Area . . . . . 25
2.2.2	Connectivity Modeling Framework . . . . . 25
2.2.3	Predicting Habitat Suitability . . . . . 28
2.2.4	Model Inputs . . . . . 29
2.2.5	Summarizing Current Flow Maps . . . . . 35
2.3	Results . . . . . 36
2.3.1	Circuitscape Inputs . . . . . 36
2.3.2	Border Impacts . . . . . 36
2.3.3	Present-day Connectivity . . . . . 39
2.4	Discussion . . . . . 40
Bibliography . . . . .	43

Appendix A	.....	55
A.1	JaguarData.info Selection Criteria .....	55
A.2	Bayesian Directed Acyclic Graph .....	55
A.3	Riparian Vegetation and Water Classification .....	56
A.3.1	Training Data Collection .....	56
A.3.2	Image Classification .....	57
A.3.3	Post Processing of Riparian Vegetation .....	58
A.3.4	Validation .....	58
A.4	Integrated Likelihood .....	60
A.5	Variogram .....	61
Appendix B	.....	62

## LIST OF TABLES

1.1	Covariate descriptions . . . . .	10
1.2	Summary of model parameter predictions . . . . .	16
1.3	Model selection results . . . . .	17
A.1	Riparian vegetation classification confusion matrix . . . . .	59
A.2	Water classification confusion matrix . . . . .	60
B.1	Summary of resistance surface inputs . . . . .	62

## LIST OF FIGURES

1.1	Map of the Chapter one study area . . . . .	5
1.2	Habitat selection probability maps . . . . .	18
2.1	Map of the Chapter 2 study area . . . . .	26
2.2	Maps of Circuitscape model output . . . . .	37
2.3	Current flow difference maps comparing border infrastructure scenarios . . . . .	38
2.4	Graphs of increases in effective resistance between trans-border habitat patches . . . . .	39
2.5	Impacts to connectivity by conversion of vehicle barriers to pedestrian fencing . . . . .	40
A.1	Directed acyclic graph of the Bayesian integrated species distribution model . . . . .	56
A.2	Variogram evaluating spatial autocorrelation of model residuals . . . . .	61

# Chapter 1

## Integrating Presence-only and Occupancy Data to Model Habitat Selection for the Northernmost Population of Jaguars (*Panthera onca*)

### 1.1 Introduction

Species distribution models (SDMs) are a useful tool for conservation because they describe where a species may occur, as well as the environmental factors that are correlated with occurrence. These models can be used to inform management decisions, so models and their inputs must be carefully developed to reduce bias. Data for fitting SDMs are often limited for rare species. This is particularly so in cases of less-studied peripheral populations. Usually, SDMs are fit with one of two types of data: presence-only records, or occupancy (detection/non-detection) data.

Presence records typically have broad coverage in geographic space. This translates to better coverage of a species' distribution, and therefore more generalizable results; however, models fit to these data may suffer from spatial sampling bias due to the lack of a formal sample design. Models using presence-only data are also unable to infer species prevalence due to a lack of information on species absence (Ward et al. 2009). This translates to biased predictions of intercept parameters in regression-based SDMs and the inability to predict actual probabilities of use (instead interpreting model predictions as the relative probability of use) (Manly et al. 2007).

Occupancy data are the most commonly-employed alternative to presence-only data. The planned survey design and repeated visits to sample units characteristic of these data offer higher information content relative to presence-only data. Repeated sampling imparts information on absence by granting the ability to adjust for observation error, that is, false negatives. Model predictions are then actual, not relative, probabilities of use, which in turn allows for the prediction

of overall prevalence. However, inference from occupancy data may still be limited by relatively narrow data coverage in geographic space due to the cost of collecting occupancy data.

Methods have been developed and applied to integrate multiple independent datasets of different types into a single model (see Hanks et al. 2011, Dorazio 2014, Giraud et al. 2016, Fletcher et al. 2016, Williams et al. 2017, Koshkina et al. 2017, for relevant applications). In an integrated model, the data and/or process models for each data type share at least one parameter. This allows the model to borrow strength from both datasets for prediction of shared parameters. A joint likelihood, derived by multiplying the individual likelihoods for each dataset, is used to evaluate the likelihood of model parameters conditional on two or more datasets. This approach yields improved inference (Illian et al. 2013, Koshkina et al. 2017). By combining two or more data types in one model, the strengths of each are leveraged while the weaknesses are offset. In SDM applications, the small geographic extent of occupancy data is offset by the broad extent of the presence-only data, while the low information content of the presence-only data is offset by the high information content of occupancy data. Integrated models offer a way to improve inference and predictions for species for which data are limited. Integrated SDMs remain relatively less explored, and opportunities exist to further develop methods for integrating occupancy and presence-only data.

Integrated SDMs have been developed by Dorazio (2014) and Koshkina et al. (2017). The models used in these studies are based on inhomogeneous Poisson point process models for presence-only and occupancy data. A Poisson point process model for presence-only data can be approximated closely via a logistic regression with a sufficient number of background points. Additionally, it is possible to account for observations errors in the background data by incorporating occupancy data in the logistic regression framework. A logistic regression-based approach provides a straightforward and approachable alternative to the Poisson point process model, particularly when integrating multiple datasets.

The jaguar (*Panthera onca*) is a species for which data are limited. Data sparsity is particularly pronounced for the northernmost extent of the species' distribution. Presence-only data for

the northernmost jaguar population are available across a broad geographic extent, but reliable, recent location records are few in number. Occupancy data are also available, but these data only exist for a small subset of the population's overall range. Novel methods for fitting integrated species distribution models provide an opportunity to improve inference and prediction of habitat selection/suitability relationships and better inform conservation.

Jaguars are classified as near-threatened by the International Union for Conservation of Nature (IUCN); however, jaguar populations in every region except the Amazon would be classified as endangered or critically endangered according to IUCN listing criteria and methodology if evaluated individually (de la Torre et al. 2018). Jaguars have been extirpated from much of their historic northern range as a result of widespread habitat loss/fragmentation, hunting, and poaching (Sanderson et al. 2002). The species is listed as endangered in the United States (US Fish and Wildlife Service 1997) and Mexico (Secretaría de Medio Ambiente y Recursos Naturales 2010).

Jaguars historically occupied most of Sonora and western Chihuahua, Mexico, as well as parts of California, Arizona, New Mexico, and Texas in the US (Hock 1955). Local populations within a larger metapopulation have been extirpated from California, New Mexico, Texas, and much of Mexico, and today may occupy only a portion of remaining structurally-suitable habitat (Menke and Hayes 2003, Hatten et al. 2005, McCain and Childs 2008, Valdez et al. 2019). Accurate predictions of habitat suitability, such as those made via an SDM, are critical for informing targeted management action for connectivity, recolonization, and habitat protection.

Several studies have mapped jaguar habitat in northern Mexico and the Southwest US (Menke and Hayes 2003, Boydston and González 2005, Hatten et al. 2005, Grigione et al. 2009, Sanderson and Fisher 2011). Models developed by Sanderson and Fisher (2011) were used to directly inform critical habitat designations (US Fish and Wildlife Service 2013). These models have been foundational to jaguar conservation efforts, but these efforts can be built upon and improved. Previous models were typically at a coarse spatial resolution ( $\leq 1$  km), used historical/imprecise jaguar sighting records, relied on expert opinion, were not modeled with uncertainty, and/or did not compare competing models in a statistical framework.

Integrated modeling approaches can be used to develop an improved SDM for jaguars. The goal for this study was to provide detailed and accurate information on the spatial distribution of habitat for the northernmost population of jaguars using the sparse data that are available. I worked to meet the following objectives: (1) develop an integrated model that uses presence-only and occupancy data to generate spatial predictions of actual, rather than relative probabilities of habitat use, (2) develop and compare competing models of habitat selection by considering important ecological processes and jaguar life history characteristics, and (3) analyze the spatial distribution of habitat based on the best-performing model to inform discussions and decisions about conservation priorities for jaguars in their northern range.

## **1.2 Methods**

Our approach for this study was as follows: 1) define the study area and obtain jaguar presence-only and occupancy records, (2) identify and generate covariate data, (3) compare different models in a model selection framework, and (4) make predictions of habitat quality throughout the study area.

### **1.2.1 Study Area**

The study area was defined by the northern portion of the jaguar's historical range in Sonora and Chihuahua, MX and southern Arizona and New Mexico, USA (see Figure 1.1), and was delineated to include portions of the historical jaguar range north of Interstate 10 in the US (Figure 1.1). The study area primarily consisted of vegetation communities of lowland desert, Madrean oak and pine-oak woodlands, pine forest, thornscrub, and tropical dry forest. Elevation ranges from sea-level to 3482 m.

### **1.2.2 Data**

The presence-only data used in this study were obtained from the Jaguar Observations Database (Wildlife Conservation Society 2015) using selection criteria to include only reliable observation

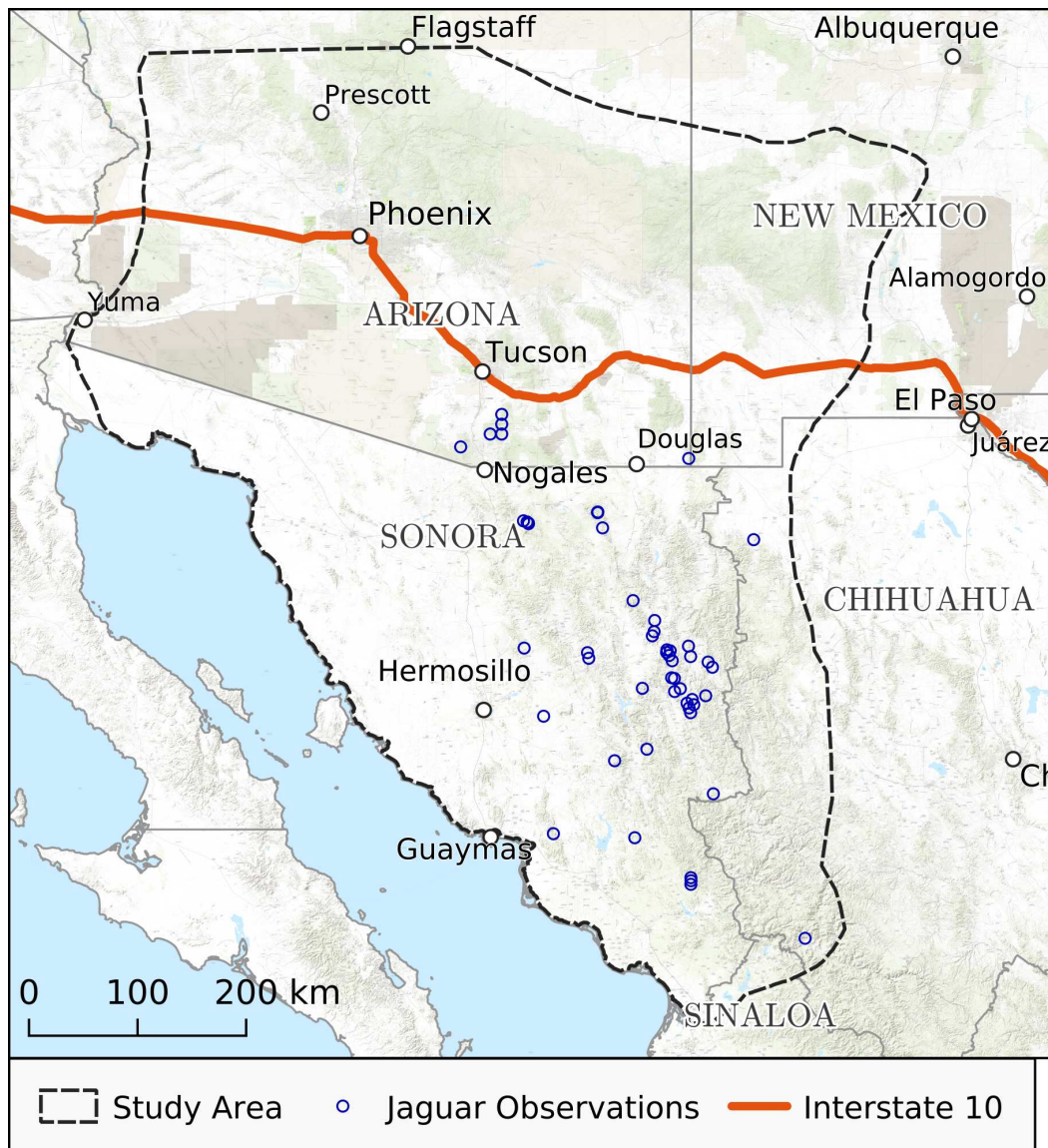


**Figure 1.1:** The study area extent with jaguar presence points and US Interstate 10 overlaid.

records after January 1st, 1985, the first year for which a complete record of Landsat 5 imagery is available. The inclusion criteria are detailed in Appendix A.1. After removing redundancies in the data, this resulted in 43 data points. Thirteen additional data points were obtained from the Madrean Archipelago Biodiversity Assessment (MABA) database (Sky Island Alliance 2019) after filtering to include only first-hand records after January 1st, 1985.

For the presence-only component of the model, background points were generated using a simple random sample within the study area as recommended by Barbet-Massin et al. (2012). This

method, rather than sampling from a circular or Gaussian kernel around the presence points, was used because it allows for spatially explicit predictions of habitat suitability throughout the entire study area, which is the primary goal of this study. A total of 25,000 points were sampled to ensure a good characterization of the environmental covariate space in the study area (Northrup et al. 2013). Each background point was assigned a year at random in proportion to that year's representation in the presence data because some covariates varied by year.

Occupancy data were collected in a total of 288 sites in a 400 km<sup>2</sup> area in the rural municipality of Nácori Chico, located in northeastern Sonora 175 km south of the U.S.-Mexico international border. Digital remote cameras (Cuddeback- Excite-Non Typical Inc., Park Falls, Wisconsin, USA) were placed throughout two separate areas for a total of five camera trapping sessions. Two spatially non-overlapping sessions were run in a 144 km<sup>2</sup> area during August 1st - December 22nd, 2008. Three spatially non-overlapping sessions were run in a separate 169 km<sup>2</sup> area during August 1st - December 22nd, 2009. Camera locations were limited to dirt roads, game and cattle trails, and along ephemeral stream beds (arroyos) due to rugged terrain, low road density, and dense vegetation. Cameras were placed randomly along likely travel corridors at distances between 600 and 1200 m ( $\bar{x} = 910\text{m}$ ) from one another. Each camera was placed 50-70 cm above the ground and 3-4 m from the path, road, or wash. Cameras were not baited. All research was conducted under a scientific permit issued by the government of Mexico (DGVS 00776/09). Each camera trap was left for up to seven 7-day sampling occasions.

### **1.2.3 Integrated Species Distribution Model**

Building upon integrated SDMs developed by Dorazio (2014) and Koshkina et al. (2017), I developed an integrated model that uses presence-only and occupancy data to predict a resource selection probability function (RSPF; *sensu* Manly et al. 2007). The model was applied in a Bayesian hierarchical framework and can be broken into two components: an occupancy model (MacKenzie et al. 2002) and a presence/background model (*sensu* Manly et al. 2007). The chosen spatial unit of inference (30×30 meter pixel for this study) is smaller than the focal organism's home range and

thus violates the closure assumption of occupancy models, as is true for many occupancy studies of large mammals. Therefore, what would normally be interpreted as an occupancy probability is instead interpreted as a use probability since individual animals will not necessarily occupy a single pixel for the duration of the study. The model is described in mathematical form below. See Figure A.1 in Appendix A.2 for a directed acyclic graph (DAG) representation of the model.

The occupancy model component was implemented with a fixed-effects regression on the probability of use ( $\psi_i$ ) assuming a homogeneous detection probability ( $p$ ). The response variable,  $y_i$ , is defined as the number of detections out of a total of  $n_i$  sampling occasions for site  $i$  ( $i = 1, 2, \dots, 288$ ), and  $z_i$  is the unobserved use state for site  $i$ .

$$y_i \sim \begin{cases} 0 & , z_i = 0 \\ \text{binomial}(n_i, p) & , z_i = 1 \end{cases} \quad (1.1)$$

$$z_i \sim \text{Bernoulli}(\psi_i) \quad (1.2)$$

$\psi_i$  is the probability of use for occupancy site  $i$  and is defined by a vector of site-level covariates  $\mathbf{x}_i$  (the first of which being 1, for the intercept) and a vector of regression coefficients  $\beta$  as follows:

$$\text{logit}(\psi_i) = \mathbf{x}_i' \beta \quad (1.3)$$

The presence/background model component is based on a use-available resource selection function (RSF; *sensu* Manly et al. 2007) and modified to include a sampling probability  $b$  (described in further detail below) that allows for the prediction of an actual, rather than relative, probability of use,  $\psi_j$ . The response variable,  $w_j$ , for this model is the observed use state for site  $j$  ( $w_j = 1$  if site  $j$  is an observed presence and 0 if site  $j$  is a background location).

The data used for this model include a sample of used sites ( $w_j = 1$ ) observed without error and a sample of background sites ( $w_j = 0$ ) with use-states ( $z_j$ ) that are observed imperfectly with possible false negative errors. I incorporated the parameter  $b$ , describing the sampling probability

to account for false negative errors, often referred to as contamination.

$$b = \Pr(w_j = 1 | z_j = 1) \quad (1.4)$$

Although the parameter  $b$  is normally not identifiable in a resource selection function, it is identifiable in this case due to the incorporation of occupancy data in the first model component. Therefore, contamination of the background sample (background sites for which the unobserved true use state is 1) can be accounted for by the model.

The addition of a parameter for sampling probability,  $b$ , forms the following distribution for the data model on  $w_j$ .

$$w_j \sim \text{Bernoulli}(\psi_j b) \quad (1.5)$$

as

$$\psi_j b = \Pr(z_j = 1) \times \Pr(w_j = 1 | z_j = 1) \quad (1.6a)$$

$$= \Pr(w_j = 1 \cap z_j = 1) \quad (1.6b)$$

$$= \Pr(w_j = 1), \text{ as } w = 1 \text{ is a subset of } z = 1 \quad (1.6c)$$

where

$$\text{logit}(\psi_j) = \mathbf{x}'_j \boldsymbol{\beta} \quad (1.7)$$

The two model components are linked through the shared regression coefficient parameters  $\boldsymbol{\beta}$ . The integration of these two models yields the joint likelihood:

$$[\mathbf{y}, \mathbf{w} | \mathbf{z}, b, p, \boldsymbol{\beta}] = \prod_{i=1}^n [y_i | p, \mathbf{n}_i]^{z_i} 1_{\{y_i=0\}}^{1-z_i} [\mathbf{z}_i | \mathbf{x}_i, \boldsymbol{\beta}] \times \prod_{j=1}^m [w_j | \mathbf{x}_j, \boldsymbol{\beta}, b] \quad (1.8)$$

## Priors

Vague normal priors (mean = 0, sd = 1.5) were used for regression coefficients  $\beta$  (Hobbs and Hooten 2015). A beta prior was used for detection probability,  $p$ , with shape parameters informed by available prior information from two studies (Sollmann et al. 2012, Gutiérrez-González and López-González 2017). Assuming detection does not vary within the sampling period, daily detection probabilities for each of the two studies were derived and used to calculate the detection probability for the 7-day sampling period used in this study. A weighted average of the detection probabilities from these studies was used as the mean of the beta prior on  $p$ . Because the study by Gutiérrez-González and López-González (2017) occurred in proximity to the occupancy survey used for this study, their estimate of  $p$  was weighted at 60% and the other study's estimate was weighted at 40%, for a mean of 0.154. A standard deviation of  $0.51\bar{3}$  (coefficient of variation of  $3.\bar{3}$ ) was used to reduce the probability density of values close to zero. This resulted in a beta prior with an alpha shape parameter of 7.46 and a beta shape parameter of 40.982 using moment matching (Hobbs and Hooten 2015). For  $b$ , a vague beta prior was used with alpha and beta shape parameters both set to one (i.e. a uniform 0-1 distribution).

### 1.2.4 Landscape Covariates

The covariates considered for jaguar habitat selection models are summarized in Table 1.1 and described below. Covariates were chosen to represent factors known or hypothesized to be correlated with jaguar habitat suitability. These factors included terrain morphology (de la Torre and Rivero 2019, Hatten et al. 2005, Sanderson and Fisher 2011), distance to water (Cavalcanti 2008), presence of riparian vegetation (Rosas-Rosas et al. 2010), and human influence (Sanderson and Fisher 2011) (measured for this study as distance to roads and distance to human settlements). All covariate development was done in Google Earth Engine (Gorelick et al. 2017) unless otherwise specified, and all covariates were standardized prior to the regression analysis.

Metrics of terrain ruggedness and NDVI were each calculated using circular moving windows and compared for three different radii (1080 m, 2160 m, and 3240 m).

**Table 1.1:** Summary of covariate layers used for species distribution modeling.

<b>Covariate</b>	<b>Description</b>	<b>Source</b>	<b>Resolution</b>
Terrain Ruggedness (TR)	Neighborhood standard deviation of the Continuous Heat Insolation Load Index (CHILI; Theobald et al. 2015)	ALOS DEM	30 meters
Normalized Difference Vegetation Index (NDVI)	The neighborhood mean of the annual median NDVI for the year corresponding to the data point	LANDSAT 5, 7, 8	30 meters
Distance to roads (road)	Euclidean distance to the nearest road	OpenStreetMaps (2017)	30 meters
Distance to built-up/human settlement (sett)	Euclidean distance to the nearest “built-up” pixel	Human Built-up And Settlement Extent (ca. 2010)	30 meters
Distance to riparian vegetation (rip)	Distance to the nearest riparian pixel predicted from a supervised classification using a random forest algorithm	Sentinel 2 (2016-2017); ALOS DEM	10 meters
Distance to water (water)	Distance to the nearest water pixel predicted from a supervised classification using a random forest algorithm	Sentinel 2 (2016-2017); ALOS DEM	10 meters

Terrain ruggedness was calculated based on the Continuous Heat Insolation Load Index (CHILI; Theobald et al. 2015). CHILI was calculated using the ALOS DEM (Tadono et al. 2014) at 30 meters resolution. To characterize ruggedness, I applied a moving window to calculate the neighborhood standard deviation of CHILI. CHILI is primarily a function of both slope and aspect, and topography is entirely a function of these two characteristics. The rationale for using the neighborhood standard deviation as a metric of terrain ruggedness was that more variation among CHILI values in a neighborhood means that there is more variation among slope and aspect, which means the terrain in the surrounding area is generally more rugged.

The normalized difference vegetation index (Rouse et al. 1974) was included as a covariate to represent the total amount of cover available in a region. To calculate NDVI, LANDSAT images were compiled for the year corresponding to the data point. Clouds were masked using the quality assurance (QA) bands available in the images. The resulting cloud-free images were used to calculate a median NDVI value for the given year for each pixel. Habitat selection is likely influenced

not only by an individual pixel, but also the pixels around it, so a circular moving window was applied as described above to calculate the mean neighborhood NDVI value for the annual cloud-free median NDVI image.

I considered three different radii at which to measure terrain ruggedness and NDVI due to uncertainty associated with the neighborhood scale that is most relevant for predicting jaguar habitat selection. One of the three radii was chosen for each covariate by visually inspecting and comparing the distributions of covariate values for used vs. background points. The scale that yielded the most obvious differentiation between used and background points was chosen as the analytical scale for that covariate. For terrain ruggedness, the greatest differentiation occurred at a radius of 3240 m, and for NDVI, the greatest differentiation occurred at 2160 m.

Raster layers of riparian vegetation and water were created using supervised classification of a multi-band image consisting of sentinel 2 bands (Drusch et al. 2012) and derivations thereof, as well as topographical bands derived at 30 m resolution from the ALOS DEM (Tadono et al. 2014). Classifications predicted out-of-sample validation data with high overall accuracies: 92% for riparian vegetation, and 95% for surface water. Supervised classification was performed in Google Earth Engine, and layers for the distance to water and distance to riparian vegetation were created in ArcMap 10.3 (Environmental Research Systems, Inc. (ESRI) 2014). Additional detail on the methodology used to derive these layers is available in Appendix A.3.

To characterize the degree of human influence on the landscape, I used the Human Built-up And Settlement Layer (HBASE; Wang et al. 2017). I created a binary raster of built-up areas from HBASE. Roads were not included as they were considered as a separate covariate in the regression analysis. From the resulting binary raster, I calculated the Euclidean distance to the nearest settlement. For the final covariate layer, distance was log-transformed to reflect that distance typically only has an ecological impact when relatively close to built-up areas.

Distance to the nearest road was calculated at 30 meters resolution using filtered OpenStreetMaps roads data (OpenStreetMap contributors 2017). Prior to calculating distance, roads were filtered

to include only major road types<sup>1</sup> because jaguars have been known in some cases to travel along or be relatively unaffected by minor dirt roads (Crawshaw Jr et al. 2004). The “residential” road class was excluded prior to analysis as well because this class is assigned inconsistently throughout the study area (e.g. some dirt roads in national forests are classified as residential). Distance to road was log-transformed to reflect the hypothesis that roads have diminishing impacts on habitat selection as distance is increased.

The model as formulated requires the assumption that all covariates were observed without error, which clearly is not the case. Inferences about model uncertainty will be optimistic relative to inferences based a model where errors in observations of covariates are properly modeled.

### **1.2.5 Model Fitting**

Models were fit using a Markov chain Monte Carlo (MCMC) sampler coded in R (R Core Team 2019). Samplers were run on seven chains in parallel, each with 12500 samples. The first 2500 samples of each chain were discarded as burn in. Convergence was evaluated using the potential scale reduction factor (PSRF; Gelman et al. 1992). All seven chains were combined after discarding burn in for a total of 70,000 samples to ensure a sufficient characterization of posterior distributions of model parameters.

### **1.2.6 Model Selection**

I developed competing models using all possible combinations of covariates after excluding any models that contained two or more covariates that had a correlation greater than 0.5. This resulted in 33 models in total. Models were scored using a Deviance Information Criterion (DIC; Spiegelhalter et al. 2002) based on an integrated likelihood (see Appendix A.4) in which the partially-observed state  $z$  for the occupancy component of the model is integrated out of the likelihood and the ability of the top-level parameters ( $p$ ,  $b$ , and  $\beta$ ) to predict the data is evaluated. DIC is not

---

<sup>1</sup>“Motorway”, “Trunk”, “Primary”, “Primary\_link”, “Secondary”, or “Secondary\_link” road types

typically suitable for mixture models, but the integrated likelihood approach ameliorates this issue (Celeux et al. 2006).

### 1.2.7 Model Validation

Predictions of habitat suitability were evaluated according to Boyce et al. (2002). The Boyce Index is traditionally calculated using the Spearman-rank correlation (Spearman 1904) test carried out in a frequentist (i.e. non-Bayesian) framework. The Spearman rank correlation test evaluates the degree of correlation between the ranks of two variables. This method is applied to evaluate the fit of SDMs fit to presence-only data by binning a habitat map produced by the SDM into discrete classes, identifying the number of data points that fall into each category, and calculating the Spearman rank correlation between the bin number and the number of points in each bin. A high correlation,  $\rho$ , indicates good model fit, and a low correlation indicates poor model fit.

A frequentist test of correlation (like the Spearman rank test of correlation) was not appropriate for this study because all analyses were carried out in a Bayesian framework. I used a Bayesian implementation of a correlation test provided by Bååth (2014) that assumes a bivariate t distribution for the two variables of interest and predicts their correlation.

Each pixel's mean habitat selection probability was calculated using 10,000 MCMC samples, and the resulting map was used for validation exercises. I binned the habitat map into 10 approximately equal area classes and recorded the number of points that fell in each bin for both the presence-only data used for model fitting as well as out of sample home range movement data for two jaguar individuals (from Morato et al. 2018). I adjusted the number of points in each bin by the bin's area (Boyce et al. 2002). Each bin was given an integer rank of 1-10 in order of increasing habitat selection probability values, and the corresponding number of points in each bin were ranked, 1-10, in ascending order following Boyce et al. (2002). I predicted correlation between those ranks to obtain a Bayesian version of the Boyce Index.

### 1.2.8 Mapping and Analysis of Habitat

Modeling in a Bayesian framework allows for predictions of both the mean and standard deviation of habitat selection probability (hereafter referred to as habitat suitability) on a pixel-level basis. After model convergence, each sample from the MCMC sampler can be considered a prediction of parameters for the model conditional on the data. I took a random sample ( $n=10,000$ ) from 70,000 total MCMC samples of regression coefficients for the top-performing model based on DIC and used these model predictions to generate 10,000 habitat maps of over 530 million pixels each in Google Earth Engine. The resulting habitat maps were used to calculate the mean and standard deviation of habitat selection probability for every pixel.

The habitat map is on the probability scale (i.e. each pixel has a value from 0-1 describing its probability of selection), so one can simply sum the pixel probabilities multiplied by their corresponding area to get a prediction of the total area of used (or usable) habitat conditional on the data. Densities of jaguars throughout the study area are likely lower than carrying capacity might allow, so this metric likely underestimates the total area of suitable habitat in the study region. Jaguars currently present on the landscape may only be using the highest-quality habitats, with relatively lower-quality (but still suitable) habitats remaining unoccupied. Ultimately, this impacts the model parameter predictions (particularly the intercept,  $\beta_0$ ), which results in lower probabilities of use across the study area on average. Consequently, an estimate of habitat amount using this methodology should be interpreted as the total amount of usable habitat based on jaguar prevalence during the sampling period within the camera trap survey area.

For calculating total area of habitat only 5,000 posterior samples were used due to computational constraints. To obtain estimates of total habitat in the study area, I created 5,000 habitat selection probability maps corresponding to 5,000 MCMC samples of regression coefficients and calculated the sum of probabilities for each map within the total study area and subsets of it. I obtained the mean and corresponding 95% Bayesian credible intervals (BCI) using the 5,000 predictions.

### 1.3 Results

Based on the top model there is 25,463 km<sup>2</sup> (95% equal-tailed Bayesian Credible Interval (BCI): 14,323-41,730) of habitat in the study area. The United States makes up 38.9% of the area in the study region, and 40.6% (BCI: 38.3-43.3%) of suitable habitat is in the US portion of the study area. 85.9% (BCI: 81.4-88.0%) of the total habitat in the U.S. is predicted to be north of I-10, while ~66% of the total area in the US portion of the study area lies north of this highway.

The best model predicted habitat selection to be positively associated with terrain ruggedness, and negatively associated with terrain ruggedness squared and distance to riparian vegetation. Mean predictions and associated 95% equal-tailed Bayesian credible intervals for model parameters are shown in Table 1.2. The quadratic relationship between terrain ruggedness and habitat selection probability shows that habitat suitability increases as terrain ruggedness increases, but begins to decrease as terrain ruggedness approaches extremely high values. A terrain ruggedness value at the 0.921 (BCI: 0.843-0.999) quantile of the distribution of terrain ruggedness values through the study area yields the highest habitat selection probability when distance to riparian is held at its mean.

A variogram for the residuals of model predictions for the presence/background data used for model fitting is provided in Figure A.2. There is some evidence that there is spatial structure in the process that is not accommodated by the model, but it is not strong.

Maps of mean predicted selection probability and coefficient of variation are shown in Figure 1.2. In the southern portion of the study area, regions of high selection probability are generally more contiguous than in the northern portion. Large regions of poor quality habitat in flat arid regions surround relatively isolated patches of good habitat in mountainous regions between the international border and US Interstate 10. The prediction for the intercept  $\beta_0$  ( $-4.327$ ; BCI:  $-5.362, -3.349$ ) is very low, which translates to low jaguar prevalence throughout the study area. The sampling probability,  $b$ , was also low (0.047; BCI: 0.025, 0.081), meaning that a large number of points in the background sample (relative to the number of presence points, 57) were false negatives.

**Table 1.2:** Mean predicted parameter values and associated 95% equal-tailed Bayesian credible intervals (BCI) for the top-performing model. TR: Terrain Ruggedness; rip: Distance to riparian vegetation

<b>Parameter</b>	<b>Mean</b>	<b>Standard Deviation</b>	<b>95% BCI</b>
$\beta_0$	-4.212	0.505	[-5.221, -3.248]
$\beta_{\text{TR}}$	2.800	0.582	[1.730, 3.991]
$\beta_{\text{TR}^2}$	-0.918	0.289	[-1.495, -0.359]
$\beta_{\text{rip}}$	-1.114	0.608	[-2.441, -0.103]
$b$	0.043	0.013	[0.023, 0.075]
$p$	0.137	0.031	[0.082, 0.203]

The best-performing models consistently included terrain ruggedness (Table 1.3). Covariates for distance to riparian vegetation and distance to water were highly correlated ( $\rho = 0.73$ ), so no models including both of those covariates were evaluated. Models with distance to riparian vegetation as a covariate performed better according to DIC than comparable models that included distance to water (Table 1.3). Models that did include distance to water predicted consistent negative effects of increasing distance to water on habitat suitability. All models had PSRF values of less than 1.05 for all parameters, indicating convergence (Gelman et al. 1992). Validation exercises show reasonable model performance for the top model, with rank correlations of 0.83 (BCI: 0.50-0.98) for out-of-sample home range movement data and 0.73 (BCI: 0.26-0.97) for the presence-only data used in model fitting.

## 1.4 Discussion

### 1.4.1 Habitat Modeling

This work provides the first parametric statistical model of habitat suitability for the northernmost population of jaguars. The methods developed provide a novel approach to integrated species distribution modeling that provides a simple, reliable alternative to the Poisson point process approach used in the past (e.g. Dorazio 2014, Koshkina et al. 2017).

**Table 1.3:** Deviance Information Criterion (DIC) for the 10 best-performing models. TR: terrain ruggedness; NDVI: Normalized Difference Vegetation Index; sett: log-transformed distance to settlement; rip: distance to riparian vegetation; road: log-transformed distance to road; water: distance to water.

<b>Model</b>	<b>DIC</b>
TR + TR <sup>2</sup> + rip	741.02
TR + TR <sup>2</sup> + sett + rip	741.90
TR + TR <sup>2</sup> + road + rip	742.64
TR + TR <sup>2</sup> + water	743.44
TR + TR <sup>2</sup> + NDVI + sett + rip	743.44
TR + TR <sup>2</sup> + NDVI + rip	743.51
TR + TR <sup>2</sup> + sett + water	744.23
TR + TR <sup>2</sup> + NDVI + water	744.32
TR + TR <sup>2</sup> + NDVI + road + rip	745.28
TR + TR <sup>2</sup> + road + water	745.56

Bayesian rank correlation tests for both the presence-only data used for model fitting as well as withheld home range movement data suggested reasonable model fit. The top model appears to be predictive of both 2nd order (home range) and 3rd order (within home range) selection (Johnson 1980) based on the correlation tests with both presence and home range movement data. The predicted rank correlation for the presence only data is somewhat low, but also has a very high degree of uncertainty, with posterior density at correlations at and above 0.9, but also below 0.4. This is most likely because there were so few presence points ( $n = 57$ ) used for model fitting. Contributing to the low predicted correlation, a single presence point (a potential outlier) fell in the second lowest bin of habitat suitability. With a small sample size, ranks, and therefore results, can be extremely sensitive to outliers. For example, had this single point fallen in the 6th bin instead, the mean predicted rank correlation for the presence data would have been 0.89 instead of 0.73.

The top model had relatively few covariates, and this is likely due to the degree to which so many landscape and environmental variables are correlated with terrain morphology, which is predicted to have the largest effect on habitat selection among all covariates. Individual model co-

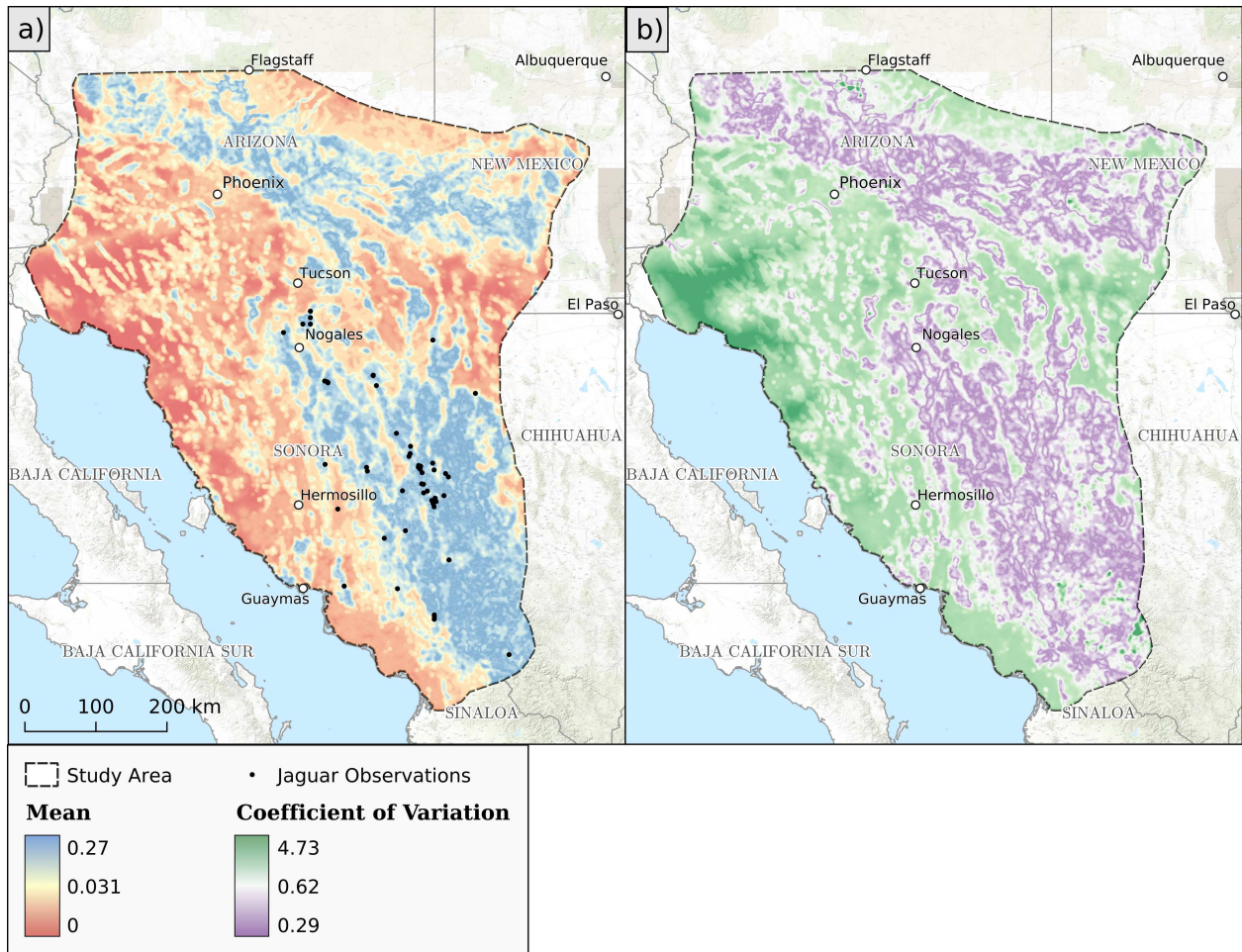


**Figure 1.2:** Maps of (a) mean predictions of probability of use with jaguar presence points overlaid, and (b) associated coefficient of variation for the predicted mean.

variables may not describe the causal process underlying habitat selection, but they are likely correlated with other factors that do. For example, despite model predictions that terrain ruggedness is positively and quadratically related to jaguar habitat selection, this does not necessarily mean that rugged areas are inherently more suitable for jaguars. This predicted relationship may be due to a variety of other factors that are correlated with terrain ruggedness. For example, terrain ruggedness is generally negatively correlated with human disturbance since high-impact land uses such as agriculture and urban, residential, and commercial development occur mainly in flat areas. Rugged areas may also provide higher prey densities due to lower human disturbance as well as better cover and water availability. Terrain ruggedness is likely predictive of habitat selection because of these factors with which it is correlated.

The prediction of habitat area throughout the study region (14,323-41,730 km<sup>2</sup>) should be interpreted as the amount of suitable habitat in the study area conditional on jaguar density in the occupancy study site, as those densities are what drove the model predictions of  $\beta_0$ , which determines overall prevalence. As such, these predictions may be biased low because of the low densities at which jaguars currently occur on the landscape. When modeling a species' distribution for a rare species, and particularly when data are sparse, the full range of environmental conditions in which the species can persist is unlikely to be represented in the data. In this case, when a fitted SDM is used to make predictions of habitat suitability in unsampled regions, the extent of suitable habitat as well as model predictions of pixel-level probabilities may be underestimated because the full domain of suitable habitat conditions is not represented by the model. This may result in additional negative bias of model predictions for total habitat area.

#### **1.4.2 Potential Conservation Implications**

Model predictions show that habitat is generally more contiguous in the southern portion of the study area than in the north. 38.9% of the study area is in the US, and 38.3-43.3% of the total area of suitable habitat lies within the US. Model predictions for the United States are generally consistent with historical observations of jaguars (see Hatten et al. 2005, Brown and López-González 2000). Large areas north of Interstate 10 remain suitable for jaguars despite being apparently unoccupied over the last 50 years. The absence of jaguars in the area may be explained by constrained dispersal from breeding populations in Sonora, which have low population densities. Barriers to movement such as highways and border infrastructure may also impede dispersal. There is limited understanding of the effects of these barriers on jaguar movement and connectivity. Enhancing this understanding emerges from my work as a high priority for future research.

Suitable habitat is relatively sparse between the international border and U.S. Interstate 10. Maintaining high-quality habitat patches in this region, along with targeted mitigation efforts to facilitate movement across highways and around border infrastructure, may improve the probability of successful dispersal to more vast regions of suitable habitat north of Interstate 10. The

projected effects of climate change on riparian vegetation in the region (Serrat-Capdevila et al. 2007) may also be of particular importance for jaguar conservation. Climate adaptation measures in riparian areas throughout the study region, as well as conservation of climate-resilient riparian corridors, may increase the probability of jaguar persistence into the future.

### **1.4.3 Integrated Species Distribution Model**

The model I developed provides a convenient and relatively simple framework to use presence-only and occupancy data jointly to model a species' distribution. This method is particularly useful in cases where data are limited and in cases where it is desirable to gain inference on species prevalence. I added an additional 288 occupancy data points from an occupancy study in a subset of the study area to gain inference on the overall prevalence of jaguars via the regression intercept. The model developed here, similarly to a Poisson point process model, allows for inference about the use state (or number of selection events) in any subregion of the study area because it is on the probability scale. When presence-only and occupancy data are both available, logistic regression and the model developed herein provides a simple (both mathematically and computationally) framework that can be readily adopted and applied in future ecological studies.

### **1.4.4 Conclusions**

Here, I described the first statistically-derived predictions of habitat selection correlates and suitability for jaguars in the northernmost portion of their range. I used a statistical model that provides predictions properly qualified by uncertainty for model parameters as well as predictions of total habitat area in the study region and its United States and Mexico portions. My modeling approach offers advantages over past efforts by considering competing models, carrying out a validation procedure, and reporting results alongside statements of uncertainty. My results provide improved inference about jaguar habitat selection and the current status of jaguar habitat in the study region, as well as robust and conservation-relevant insights into jaguar ecology. The mean predicted proportion of total habitat that lies in the US (40.6%) is similar to the proportion of the study area that lies in the US (38.9%). The roughly 40% of the total study area's habitat that lies in

the U.S could play in important role in the long term persistence of the northern jaguar population. The modeling approach described, which integrates presence-only and occupancy data in a single model, allows for improved predictions of both habitat selection and total habitat area. My study demonstrates a useful modeling framework that can be used for future applications in species distribution modeling, especially in cases where data are limited and/or there is a desire to gain inference about species prevalence.

## Chapter 2

# Trans-border Connectivity Models for Jaguars (*Panthera onca*) Reveal US-Mexico Border Wall

## Impacts

### 2.1 Introduction

Political borders are often placed arbitrarily with respect to natural boundaries, but they can have profound impacts on the natural world (see Dallimer and Strange 2015, Piekielek 2009, Lasky et al. 2011, Linnell et al. 2016, Trouwborst et al. 2016). They often have increased human activity such as border militarization or patrol activity, and/or barriers such as fencing, walls, or barricades designed to prevent illegal immigration. These characteristics, while focused on security and immigration, can have significant environmental consequences. Land use, human activity, and the infrastructure often associated with borders alter biotic (Pokorny et al. 2017, Patrick-Birdwell et al. 2013) and abiotic (Norman et al. 2010, Patrick-Birdwell et al. 2013) ecological processes and impede plant and animal dispersal.

A loss of habitat connectivity, also called habitat fragmentation (apart from habitat loss), is one of the most obvious ecological impacts of border infrastructure. Fragmentation can result in loss of genetic diversity, local extinctions (Frankham 1998), reduced carrying capacity (Herbener et al. 2012) and limited ability of species to shift their geographic ranges in response to climate change (Opdam and Wascher 2004). Examples of landscape fragmentation impacts include decreased genetic diversity in ground beetles (Keller and Largiader 2003), genetic differentiation between sub-populations of jaguars (Haag et al. 2010), long-term extinction debt (*sensu* Tilman et al. 1994) in forest plants (Vellend et al. 2006), decreased survival rates in a tropical forest bird (Ruiz-Gutiérrez et al. 2008), and altered hydrologic flows in Vietnam (Ziegler et al. 2007).

Large carnivores are among the organisms most sensitive to habitat fragmentation (Crooks et al. 2011). Their large space requirements, sensitivity to human disturbance, and slow reproductive rates make their populations particularly vulnerable to isolation. Because of their sensitivity to habitat loss and fragmentation, large carnivores can act as umbrella species to guide conservation planning when knowledge of the larger ecological system is limited (Noss et al. 1996, Rozyłowicz et al. 2011, Thornton et al. 2016). Mitigating the impacts of fragmenting barriers on large carnivore species may also have an umbrella effect, benefiting many additional species by proxy (Thornton et al. 2016). In the case of international borders and associated infrastructure designed to prevent human movement, understanding impacts on large carnivores provides foundational knowledge that can aid broader conservation efforts.

The jaguar (*Panthera onca*), a large carnivore that ranges from Argentina to the southwestern United States (U.S.) (Seymour 1989), has seen substantial range contraction over the past century owing to hunting, poaching, and habitat loss (Sanderson et al. 2002). The species is currently threatened with extinction in many parts of its range (de la Torre et al. 2018) and is particularly vulnerable to restrictions to movement. Between the U.S. and Mexico, there is extensive border infrastructure. The northernmost jaguar population historically ranged beyond Mexico and into the U.S. states of Arizona, New Mexico, and Texas (Hock 1955), but hunting and persecution by humans led to their virtual extirpation north of the U.S.-Mexico border. Jaguars are listed as endangered in the U.S. (US Fish and Wildlife Service 1997) and Mexico (Secretaría de Medio Ambiente y Recursos Naturales 2010), and a goal of both governments, as well as conservation organizations, is to facilitate jaguar dispersal from Mexico into their former range in the United States. Border infrastructure may limit the ability of jaguars to disperse into the U.S.

To date, there are at least 1000 km of pedestrian fencing and vehicle barriers along the border (Reveal from The Center for Investigative Reporting and OpenStreetMap contributors 2017). There are two primary types of border infrastructure: pedestrian fencing, and vehicle barriers. Pedestrian fencing is wall-like and typically 18-30 feet tall. It acts as an impenetrable barrier to movement by large mammals. Vehicle barriers vary widely, ranging from so-called Normandy

style barriers to concrete posts, and are typically no taller than three to four feet. Vehicle barriers typically have border patrol roads along them and increased activity from Border Patrol agents.

There is limited knowledge of the exact nature of the impacts of this infrastructure on trans-border animal movement due to the laws that facilitate its construction. In 2005, the United States passed the REAL ID act (Pub.L. 109–13, 119 Stat. 302), which expedited the construction of much of the infrastructure that exists along the U.S.-Mexico border. The law provides the Department of Homeland Security the authority to waive "all legal requirements", including local, state, and federal laws, to ensure "expeditious implementation" of border infrastructure projects (Echemendia 2009). Consequently, consideration of the environmental impacts of these projects is not required prior to or after implementation, and research into the ecological effects of border infrastructure on the environment is not mandated.

The U.S.-Mexico border wall has a substantial effect on animal movement (Peters et al. 2018). Movement, and a landscape that facilitates it, is critical for population processes such as migration, recolonization, gene flow, and range shifts, as well as individual-level processes such as foraging, dispersal, and mate searching (Crooks and Sanjayan 2006). A barrier to movement compromises all of these fundamental ecological processes.

Recently, there has been renewed interest by the U.S. government in building additional border infrastructure. The Real ID act was invoked 13 times to expedite barrier construction along the U.S.-Mexico border between January 20th, 2017 and July 2nd, 2019. Waived laws include the Endangered Species Act, the National Environmental Policy Act, the Wilderness act, and at least 25 others (Center for Biological Diversity 2019, Zazueta-Castro 2019).

Jaguars, and large mammals in general, are thought to be among those species significantly impacted by the U.S.-Mexico border and its associated infrastructure and intense human activity (e.g. from Border Patrol) (List 2007, Lasky et al. 2011, Peters et al. 2018). There is a general understanding that the border infrastructure negatively impacts jaguars because it acts as a barrier to movement, but the details and extent of these impacts remain unknown. A better understanding of

these impacts is a critical step in developing good conservation policy and management strategies for the northernmost population of jaguars.

Given the gaps in our understanding of the ecological impacts of border infrastructure on jaguars, the goal of this study was to model trans-border connectivity and quantify the impacts of border infrastructure on jaguar movement between the U.S. and Mexico. Given the recent push by the United States government to expand border infrastructure, an additional goal was to evaluate the impacts of an infrastructure expansion on jaguar habitat connectivity and movement. To accomplish the above goals, the study had the following objectives: 1) generate a connectivity model that incorporates jaguar habitat quality, land use, roads, and border infrastructure, 2) identify high-priority connectivity conservation areas given current conditions, and 3) evaluate the impacts of current border infrastructure – as well as a potential expansion – on jaguar movement by comparing three scenarios related to the border wall.

## **2.2 Methods**

### **2.2.1 Study Area**

The study area is a subset of the Chapter one study area. It spans the United States-Mexico international border region in Arizona and New Mexico, USA, and Sonora and Chihuahua, Mexico (Figure 2.1). It was delineated to include unoccupied habitat in the United States so that connectivity to those areas could be evaluated. The region is bisected into a northern and southern portion by approximately 550 km of the U.S.-Mexico international border. Within the study area there are over 200 km of pedestrian fencing, and 325 km of vehicle barriers along the border (Reveal from The Center for Investigative Reporting and OpenStreetMap contributors 2017).

### **2.2.2 Connectivity Modeling Framework**

I used Circuitscape (McRae and Shah 2009, Anantharaman et al. 2019) to model connectivity in various border wall scenarios. Circuitscape uses circuit theory to predict animal movement through a heterogeneous landscape (McRae et al. 2008). Circuitscape is built on random-walker

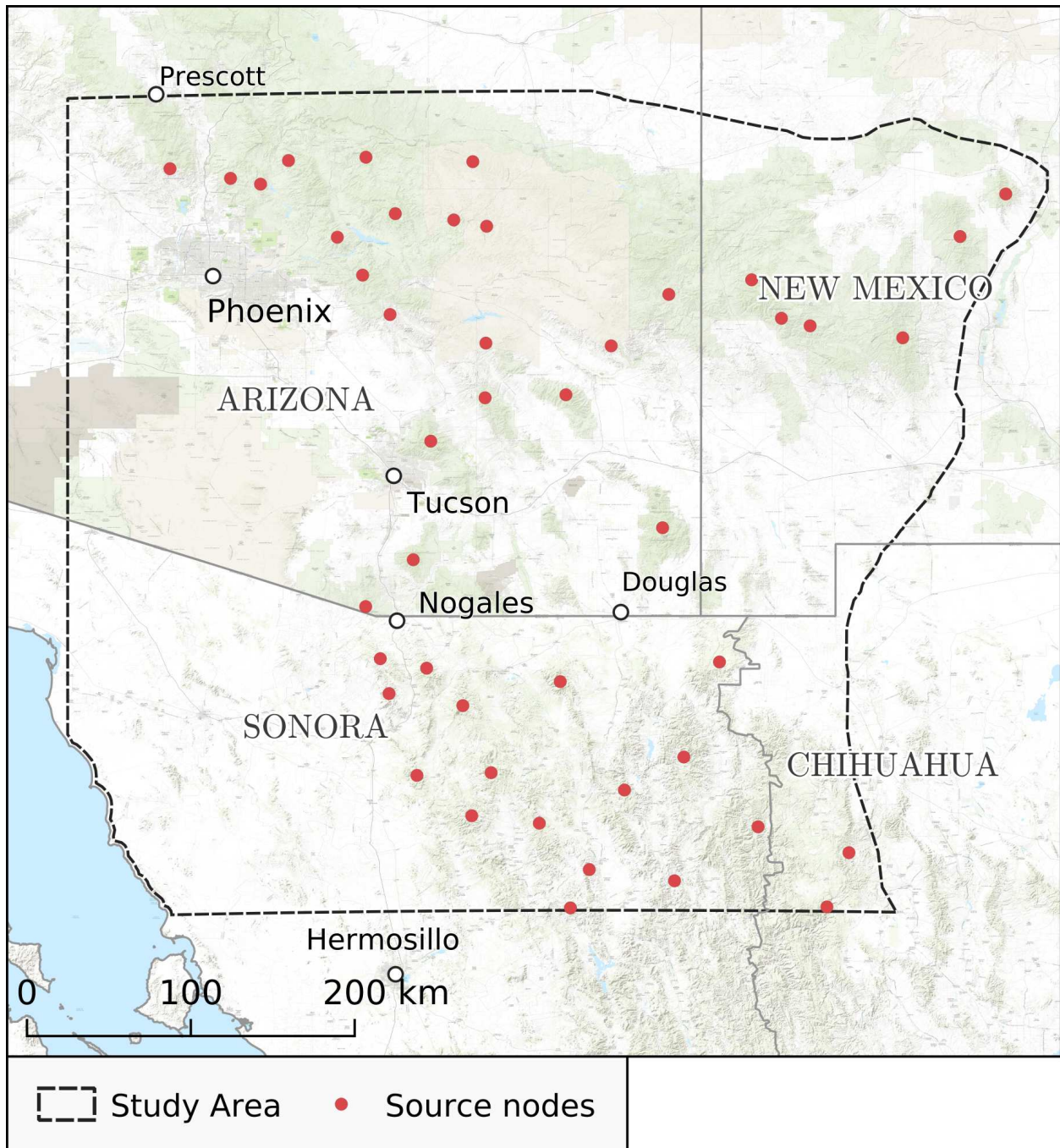


**Figure 2.1:** The study area for connectivity analyses with source nodes used in Circuitscape overlaid.

theory (McRae et al. 2008), so it is preferable to least-cost based approaches that require the assumption that dispersing animals have complete knowledge of the landscape. Jaguars dispersing north through the border region are likely to have limited knowledge of the landscape through which they are moving. First, jaguars moving from south to north would be active dispersers mov-

ing through a landscape that is novel to them because they are dispersing from breeding populations in Mexico. Second, habitat in the United States is virtually unoccupied, so intraspecific olfactory and visual cues that could be used to guide movements (Wooldridge et al. 2019) are limited. I used Circuitscape v5.5.4 (Anantharaman et al. 2019) in the Julia programming language (Bezanson et al. 2017) to leverage the improved speed and ability to handle extremely large computational problems that it offers.

Circuitscape models how electrical current flows through the resistance surface between each pair of nodes – the amount of current flowing through a region or pixel in the landscape is related to the probability that a randomly dispersing animal will pass through that region. Circuitscape provides current flow predictions and measurements of the effective resistance (i.e. the degree of isolation) between each pair of nodes. Two inputs are required to run Circuitscape: source nodes and a resistance surface. Source nodes represent current sources and grounds – the locations between which movement (current flow) is estimated. The resistance surface represents the landscape, where spatially-referenced pixels are assigned values based on their resistance to movement (in this case, movement by jaguars).

I altered the resistance surface provided to Circuitscape according to difference border infrastructure scenarios to examine the effects of each scenario on predicted current flow. I ran three landscape scenarios: 1) no border wall, (2) the present-day border infrastructure, and (3) a potential future border infrastructure expansion in which vehicle barricades are converted to pedestrian fencing. In the third scenario I focused on conversion of existing structures rather than new construction since at the time of analysis, this was the primary type of ongoing construction. I developed separate resistance surfaces for each scenario to reflect the assumptions of each. The only difference between the resistance surfaces for each scenario was the border infrastructure layer. Methods for developing nodes and resistance surface inputs for Circuitscape are described under “Model Inputs”.

A spatial data layer of predicted jaguar habitat suitability (see Chapter one) was used for developing both nodes and resistance surfaces for this analysis. I briefly describe the methods used to develop these data below.

### **2.2.3 Predicting Habitat Suitability**

To create the habitat suitability component of the resistance surface, I fit an integrated species distribution model for 2nd order (home range) habitat selection (*sensu* Johnson 1980) at 30 meters resolution. I used two datasets: a collection of presence-background data (*sensu* Manly et al. 2007), and an independently collected detection/non-detection dataset for a subset of the study area. Background points were generated randomly throughout the larger Chapter one study area, as recommended by Barbet-Massin et al. (2012). I developed competing models using all possible combinations of covariates and excluded any models that contained two or more covariates that had a correlation greater than 0.5. Models were scored using the Deviance Information Criterion (DIC; Spiegelhalter et al. 2002). Covariates considered included metrics of vegetation cover, terrain ruggedness, and proximity to human development, roads, riparian vegetation, and water.

The top performing species distribution model was used for this analysis. It included covariates for distance to riparian vegetation, terrain ruggedness, and terrain ruggedness squared. This model predicted habitat selection to be positively associated with terrain ruggedness, and negatively associated with terrain ruggedness squared and distance to riparian vegetation. I applied mean parameter estimates from this model to make predictions of habitat suitability throughout the study area and used the resulting layer as the habitat suitability map for this connectivity analysis. Further details on the methods and results for the habitat suitability analysis can be found in Chapter one.

## 2.2.4 Model Inputs

### Habitat Nodes

Nodes were defined as contiguous patches of high quality jaguar habitat suitable for a jaguar home range. To identify these patches, I used 2,193 home range movement points from Morato et al. (2018), collected from two GPS collared jaguars in northeastern Sonora. First, I calculated the average habitat suitability value within a convex polygon encompassing all of the points to identify a threshold value to convert the habitat suitability map from a continuous scale to a binary representation of habitat/non-habitat. Then, I used a 170.1 km<sup>2</sup> circular moving window to calculate the mean neighborhood habitat suitability value for each pixel in the landscape. I arrived at 170.1 km<sup>2</sup> by taking the mean home range size of 5 male jaguars in Mexico from two studies (de la Torre et al. 2017, Nuñez-Perez and Miller 2019). I converted the resulting layer into a binary representation of habitat/non-habitat using the threshold obtained from GPS collar data. I identified contiguous regions of habitat pixels in the layer. Large, irregular habitat patches were broken into separate patches. I used patch centroids, following Dickson et al. (2017), as source nodes for Circuitscape.

### Resistance Surface

I created the resistance surfaces at 120 meters resolution for each scenario using a combination of spatial data layers including the habitat suitability model (see Chapter one), human modification (*sensu* Theobald 2013), roads (OpenStreetMap contributors 2017), and border infrastructure (Reveal from The Center for Investigative Reporting and OpenStreetMap contributors 2017). These inputs are summarized in Table B.1 in Appendix B. Each layer was converted into a raster dataset, then layers were rescaled and combined to generate resistance surfaces for the three border wall scenarios outlined above. The methods for each layer are described separately below with a final section on how they were combined.

### *Habitat Suitability*

The habitat suitability map from Chapter one provides predictions of habitat suitability for jaguars in the study area at 30 meters resolution. Based on the findings of Zeller et al. (2018), I opted to use a negative linear transformation of habitat suitability to assign resistance values for this component of the resistance surface. I converted habitat suitability (HS) to resistance values,  $R_{HS}$ .

$$R_{HS} = \left( 1 - \frac{HS}{\max(HS)} \right) \quad (2.1)$$

### *Human Modification*

I incorporated potential effects of human land use on jaguar movement into the resistance surface using an estimate of human modification (HM; Theobald 2013). Human modification is a comprehensive measure of the extent and intensity of human land use on the landscape. It combines information on urban development, agriculture, energy development, and other human land uses into a single metric that ranges from zero to one (Theobald 2013). Following Kennedy et al. (2019), I estimated human modification at 300 meters resolution for the study area. I included human modification in addition to habitat suitability because general activity by jaguars in otherwise suitable habitat has been documented to decrease in response to the intensity of human activity (Foster et al. 2010). I predicted that movement is less likely to occur through these areas, despite being otherwise suitable. I set resistance,  $R_{HM}$ , equal to the HM value.

$$R_{HM} = HM \quad (2.2)$$

### *Roads*

The impacts of roads on habitat connectivity are well-documented (Forman et al. 2003). I added roads as an additional source of resistance to account for their effect on jaguar movement and connectivity. Although impacts of the road *footprint* may be incorporated via data on land cover, impacts associated with *use* (i.e. traffic) are not. I incorporated roads into the resistance

surface using road data from Open Street Map (OpenStreetMap contributors 2017). In many connectivity analyses, roads are considered to have a homogeneous effect across the study area. In reality, the degree to which a given road may act as a barrier is highly variable depending on several factors; traffic is perhaps the most important. With this in mind, I quantified the resistance of roads,  $R_{r_i}$ , to jaguar movement using average annual daily traffic (AADT) estimates adjusted by a population-weighted accessibility score (eq. 2.3). I split road geometries into segments  $\leq 2.5$  km and calculated resistance for each segment. I segmented roads to 2.5 km instead of smaller segments (e.g. 120 meters) to decrease computation time and because accessibility-weighted resistance has minimal variance within a 2.5 km segment.

I delineated settlements using the Human Built-Up And Settlement Extent dataset (HBASE; Wang et al. 2017). I retained pixels with a value of 201 (201 = Built-up, non-road). Contiguous groups of pixels were converted to polygons. Total population was calculated for each polygon using the UN-adjusted Gridded Population of the World population density dataset (GPW; Center for International Earth Science Information Network - CIESIN - Columbia University 2016). Population polygons from HBASE were often smaller than one GPW pixel (1 km<sup>2</sup>), so the GPW layer was resampled to a resolution of 30 meters prior to calculating total population. Population count per 30 meter pixel was calculated by converting the original GPW population density value (in units of people per km<sup>2</sup>) to people per meter squared. I then converted the density to a count by multiplying the density per meter squared by pixel area in meters squared. For each settlement polygon, I summed the population counts of intersecting pixels to get a final value. Only settlements with 100 or more people were retained (n = 685 settlements) to reduce computational load.

$$R_{r_i} \propto t_i \times \sum_{j=1}^n A_{ij} \quad (2.3)$$

The components of eq. 2.3 are described in detail below.

Traffic intensity ( $t_i$ ) is proportional to the predicted AADT for the road class of segment  $i$ . I made predictions of  $t_i$  for each road class type using AADT measurements from two studies in North America (Theobald 2010, Setton et al. 2005) for the following road classes: interstate/expressway, freeway/major highway, principal/major arterial, minor arterial, collector, and local. I assigned ordinal values of 1 to 6 to these classes (corresponding to the order in the list). The OpenStreetMap road data contains an additional road class, “track”, that has no AADT measurements. I assigned that class an ordinal rank of 0 for the purpose of prediction. I used the rank scores as the explanatory variable in a non-linear least-squares regression on eq. 2.4 using the nlme package (Pinheiro et al. 2018) in R (R Core Team 2019).

$$t_i = \text{AADT}_i = N_0 e^{\delta c_i} \quad (2.4)$$

$c_i$  is the ordinal rank (road class) for road segment  $i$ ,  $N_0$  is the estimated AADT for a road class of 0, and  $\delta$  is the exponential growth rate of AADT as a function of road class type. OpenStreetMaps classes were related back to the classes,  $c$ , in the regression as follows: track = 0, residential = 1, tertiary = 2, secondary = 3, primary = 4, and motorway = 5.5. The motorway class in OpenStreetMaps contains both major highways (class 5) and interstates (class 6), so I assigned it a value of 5.5 for making predictions since it is unknown whether an OpenStreetMaps “motorway” is a “major highway” or an “interstate”.

$A_{ij}$  is the population-weighted accessibility to road segment  $i$  from settlement  $j$  (eq. 2.5).  $A_{ij}$  is a function of the population size of settlement  $j$  and its distance to road segment  $i$ .  $A_{ij}$  was summed across all settlements in eq. 2.3 to account for the contributions to traffic of all settlements in and around the study area.

$$A_{ij} = A_{d_{ij}} A_{p_{ij}} \quad (2.5)$$

$A_{d_{ij}}$  (eq. 2.5) is the accessibility of segment  $i$  from settlement  $j$  based on the distance to the settlement along the road network.  $A_{p_{ij}}$  (eq. 2.5) is an adjustment to the accessibility based on the population size of settlement  $j$ . Each is described in detail below.

$A_{d_{ij}}$ , defined mathematically in eq. 2.6, has a maximum value of 1 and decreases with increasing distance,  $x_{ij}$ , along the road network between the road segment  $i$  and settlement  $j$ . I developed this approach following Theobald (2008) but opted to use a Gaussian decay of accessibility with increasing distance instead of an exponential so the effects of increasing distance would be less extreme for small distance values.

$$A_{d_{ij}} = e^{-rx_{ij}^2} \quad (2.6)$$

To calculate distance,  $x_{ij}$  in eq. 2.6, along the road network from road segment  $i$  to settlement  $j$ , I first converted the segmented road vectors into a 270 meter resolution raster representation. For each settlement, I calculated the distance along the road network to each road pixel using Google Earth Engine (Gorelick et al. 2017). For each road segment and settlement pair, I assigned a distance,  $x_{ij}$ , using the average distance between settlement  $j$  and each pixel intersecting road segment  $i$ . The decay rate,  $r$  in eq. 2.6, was defined as  $-1.732868 \times 10^{-5}$  so that  $A_{d_{ij}} = 0.5$  at a distance of 200 km along the road network from settlement  $j$ .

$A_{p_{ij}}$  adjusts  $A_{d_{ij}}$  based on the population size of settlement  $j$ . This adjustment is defined by a logarithmic function of settlement population size with parameter  $b$  (eq. 2.7).

$$A_{p_{ij}} = \log\left(\frac{P_j}{b} + 1\right) \quad (2.7)$$

I defined  $b$  as 11922.124 so that  $A_{p_{ij}} = 1$  at the mean settlement population size of 20485.57. For settlement sizes below the mean,  $A_{p_{ij}} < 1$ , and for settlements with populations larger than the average,  $A_{p_{ij}} > 1$ .

After calculating  $R_r$  for every road segment, the resulting layer was converted to a 120 meters resolution raster with values defined by  $R_r$ . Each 120 m pixel was assigned the highest  $R_r$  value

of any segments intersecting it. The resulting layer was rescaled to take a maximum value of 1 by dividing every pixel by the maximum value in the raster. This layer is proportional to the accessibility-adjusted traffic intensity.

### *Border Infrastructure*

I incorporated the border wall into the resistance surface using data from Reveal from The Center for Investigative Reporting and OpenStreetMap contributors (2017). I assigned vehicle barriers a resistance equal to 1 to match the maximum value of Human Modification. Pixels that contained pedestrian fencing were assigned a no data value, which Circuitscape interprets as an absolute barrier to movement (i.e. infinite resistance). Pedestrian fencing ranges from 18-30 ft in height, so it was assumed to be an absolute barrier to jaguar movement. To characterize the border expansion scenario in which vehicle barriers are converted to pedestrian fencing, I assigned no data values to both pedestrian fencing and vehicle barriers.

### *Combination Into Final Resistance Surfaces*

I combined the individual layers described above to create final resistance layers (at 120 meters resolution) corresponding to the three border wall scenarios: 1) no border wall ( $R_0$ ; eq. 2.8), (2) the current border infrastructure ( $R_c$ ; eq. 2.10), and (3) a potential border infrastructure expansion ( $R_e$ ; eq. 2.11). Other than the unique border infrastructure components, all three layers have identical habitat suitability, human modification, and road layers, which were combined according to eq. 2.8.  $R_r$  was multiplied by 100 so that  $R_r$  would have a maximum value 100 times larger in value (i.e. 100 times more resistant to movement) than the maximum value of  $R_{HM}$ .

$$R_0 = (1 - (1 - 0.5 \times R_{HS})(1 - R_{HM})) + R_r \times 100 \quad (2.8)$$

I combined habitat suitability and human modification resistances in eq. 2.8 using the fuzzy algebraic sum (Bonham-Carter 2014). This function provides a useful method to combine two metrics that may have additive effects, but are not completely independent. The fuzzy sum,  $q$ , of two numbers,  $w$  and  $v$  (where  $w$  and  $v$  are between 0 and 1) is show in eq. 2.9.

$$q = (1 - (1 - w)(1 - v)) \quad (2.9)$$

$R_0$  (eq. 2.8) represents the no border wall scenario. I weighted habitat suitability at 0.5 (and human modification at 1.0) so that resistance to movement could only reach 0.5 of its maximum value due to poor habitat suitability alone, but could reach its maximum value from high human modification alone.  $R_c$  (the current border wall scenario) was calculated as follows:

$$R_c = R_0 + R_{b_c} \quad (2.10)$$

$R_{b_c}$  is resistance from the current border wall scenario.

$R_e$  (an expanded border wall scenario) was calculated as follows:

$$R_e = R_0 + R_{b_e} \quad (2.11)$$

$R_{b_e}$  is resistance from the expanded wall scenario.

I ran Circuitscape in pairwise mode to model connectivity between every possible pair of nodes in the landscape. I computed maps of cumulative current flow and effective resistances between each pair of nodes for each scenario in Circuitscape.

## 2.2.5 Summarizing Current Flow Maps

I compared scenarios by calculating the differences in current between each. I did this by subtracting the output for one scenario from the output of another. I calculated two difference maps: one comparing the present-day scenario to natural conditions, and another comparing the expanded scenario to present-day conditions.

I calculated the proportion of current flow intercepted by pedestrian fencing in both the present-day and expanded scenarios to estimate how much jaguar movement would be intercepted and blocked by border infrastructure. For the present day scenario, I measured the proportion of trans-border current flow predicted under natural conditions in areas that presently have pedestrian fenc-

ing. For the expanded infrastructure scenario, I examined the impacts of border infrastructure relative to present-day and natural conditions. To compare against natural conditions, I measured the proportion of trans-border current flow predicted under the no infrastructure scenario flowing through areas that presently have pedestrian fencing *or* vehicle barricades. To compare against present-day conditions, I measured the proportion of trans-border current flow predicted under the present-day infrastructure scenario that flowed through areas with vehicle barricades. I summed the current flow values of pixels in a given current flow map (either the no-infrastructure or present-day infrastructure scenario) that were intersected by pedestrian fencing (or vehicle barriers in the case of the expanded scenario) and divided that by the sum of all border pixel current flow values to estimate the proportion intercepted.

To identify areas where connectivity would be most negatively impacted by conversion from vehicle barriers to pedestrian fencing, I split the lines representing the footprint of present-day vehicle barriers into segments  $\leq 2$  km, then calculated the amount of current flow in the present-day scenario passing through each segment. Segment lengths varied, so to make measurements directly comparable between segments, I adjusted the sum for a given segment by dividing it by the total number of pixels that segment intersected.

## **2.3 Results**

### **2.3.1 Circuitscape Inputs**

I identified a total of 45 habitat nodes (overlaid on Figure 2.1), resulting in 990 pairwise connections solved in Circuitscape. The non-linear least-squares regression for AADT by road type resulted in an estimate of 1509.868 ( $p < 0.1$ ) for  $N_0$  and 0.7044042 ( $p < 0.001$ ) for  $\delta$ . These values were used to estimate AADT by road type using eq. 2.4.

### **2.3.2 Border Impacts**

Pedestrian fencing in the present-day border infrastructure scenario (i.e. current conditions) intercepts over 21% of all trans-border jaguar movement predicted to occur under natural (i.e. no

border infrastructure) conditions. The expanded wall scenario in which vehicle barriers were converted to pedestrian fencing would block >62% of movement predicted under natural conditions, and >50% of movement predicted under present-day conditions.

Maps of current flow for each scenario considered by this study are shown in Figure 2.2. High current flow is associated with a higher probability of movement through a given pixel, and low current flow is associated with a low probability of movement. In the scenario with no border infrastructure (Figure 2.2a), trans-border current flow is generally diffuse (i.e. spread out among many different paths), suggesting multiple redundant movement pathways. With present-day border infrastructure added to the model (Figure 2.2b), trans-border current flow through the central portion of the border south of Tombstone, AZ and west of Douglas, AZ (see Figure 2.1 for reference) is diverted east and west. In the expanded border wall scenario (Figure 2.2c), trans-border current flow becomes further restricted to very narrow pathways.

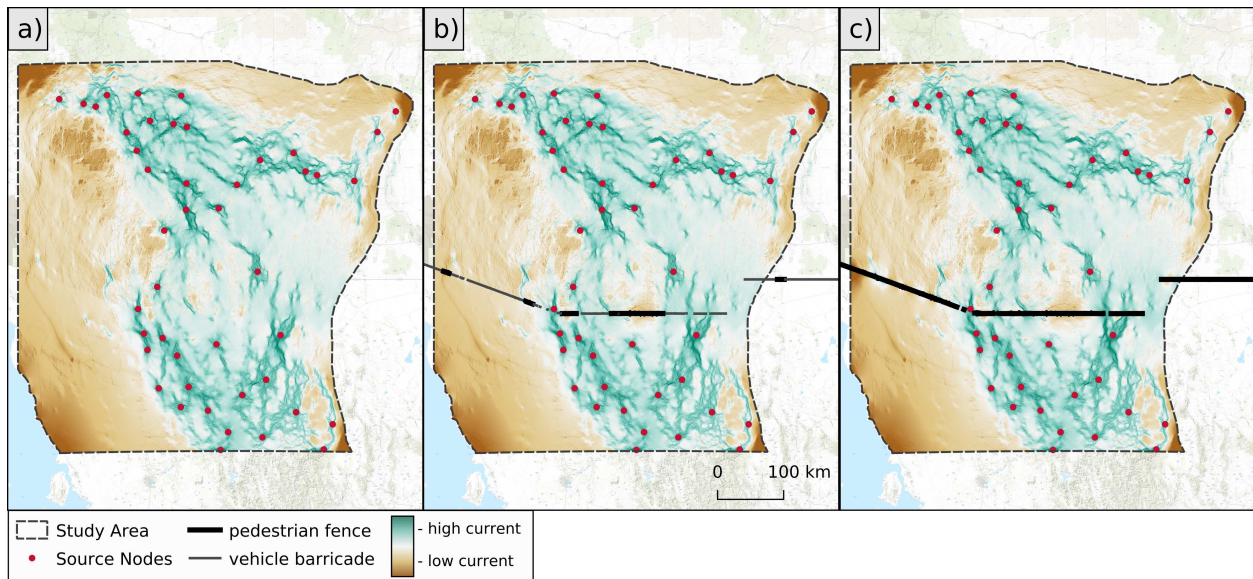


**Figure 2.2:** Circuitscape output for the three border infrastructure scenarios with the border infrastructure layers used for each scenario overlaid. Scenarios explored were: a) no border infrastructure, b) the present-day border infrastructure, and c) expanded border infrastructure. Note that small discontinuities in border infrastructure are not all visible due to the scale of the map.

Difference maps showing the impacts of present day vs. natural conditions and expanded vs. present day conditions are shown in Figure 2.3. These maps can be used to evaluate the impacts of

a given scenario by identifying areas where there are increases or decreases in predicted current. Both difference maps show impacts of border infrastructure on habitat connectivity extending well over 100 km from the border to the north and south.

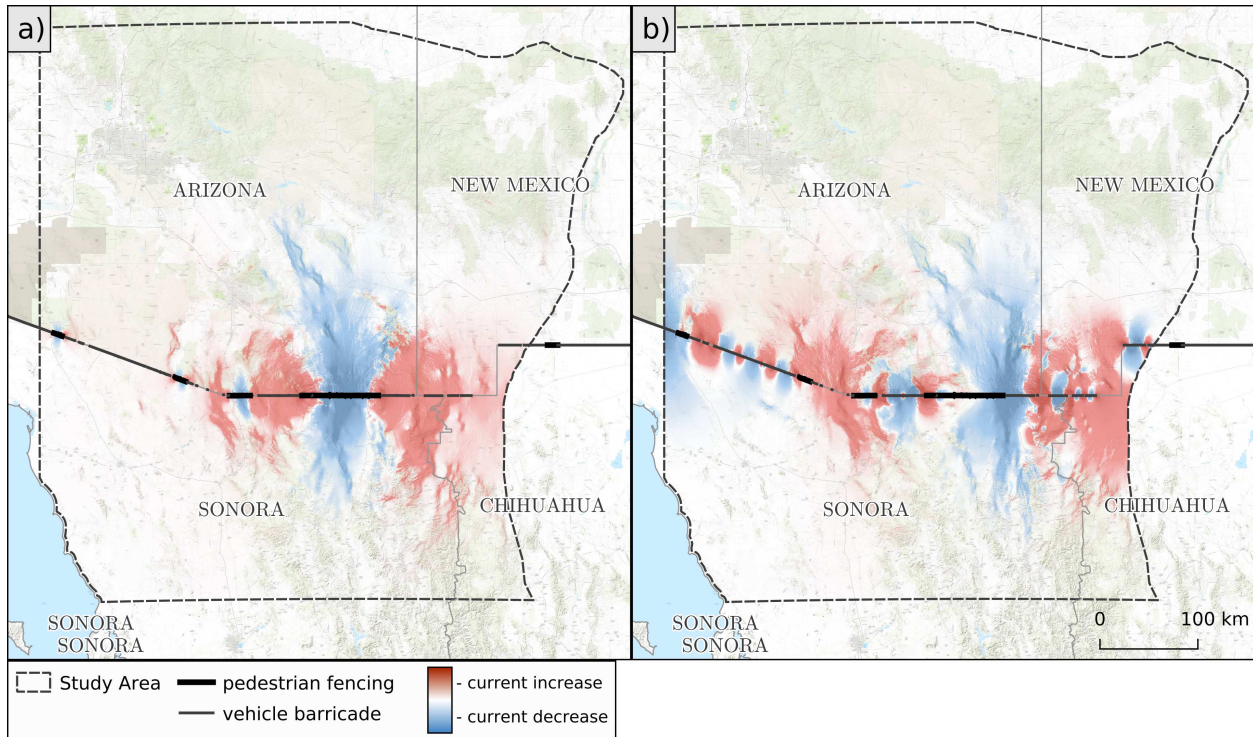


**Figure 2.3:** Current flow difference maps for a) the present-day border infrastructure scenario minus the no infrastructure scenario and b) the expanded scenario minus the current scenario. Present-day border infrastructure is overlaid on both for reference. Note that small discontinuities in border infrastructure are not all visible due to the scale of the map.

Figure 2.4 shows summaries of the number of trans-border node pairs (i.e. where one node is in Mexico and the other in the U.S.) experiencing varying degrees of increase in effective resistance (i.e. isolation; McRae et al. 2008) from one scenario to another. Certain node pairs experience increases in effective resistance of nearly 20%. Note that increases in effective resistance between points A and B have a positive correlation, but do not necessarily scale linearly with the probability of a jaguar successfully dispersing from point A to point B. An increase of 5% in the degree of isolation could mean a 50% (or 1%) decrease in dispersal probability. Comparing Figure 2.4c to Figure 2.4a shows that the expanded border infrastructure scenario results in a significantly

larger increase in trans-border isolation than does present-day infrastructure. The impacts of the conversion of existing vehicle barriers to pedestrian fencing on a segment-wise basis are shown in Figure 2.5.

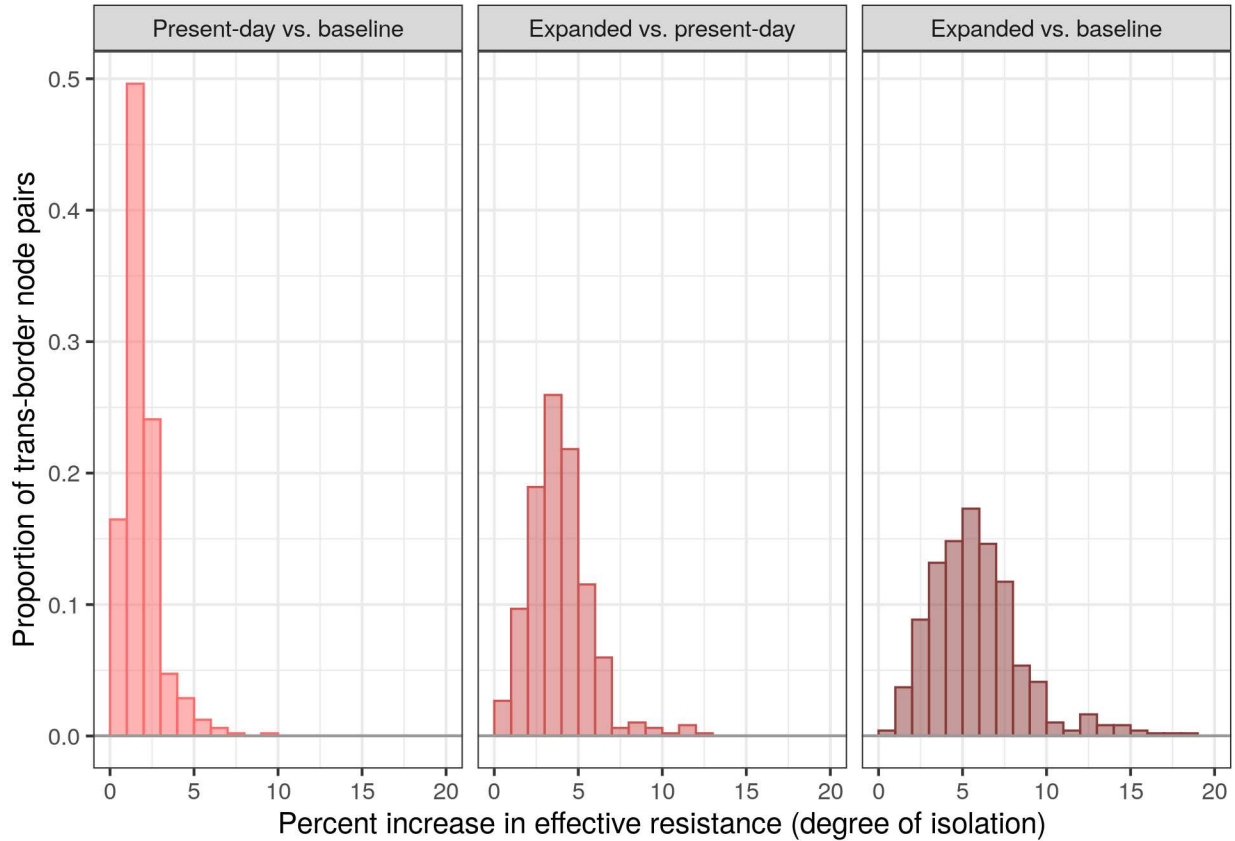


**Figure 2.4:** A plot of the proportion of trans-border node pairs experience varying degrees of increase (in percent) in effective resistance from one scenario to another. a) compares effective resistances in the present-day scenario to the baseline (no infrastructure) scenario, b) shows the same but for the expanded infrastructure scenario compared to present-day, and c) shows the same but for the expanded infrastructure scenario compared to the baseline (no infrastructure) scenario.

### 2.3.3 Present-day Connectivity

Despite the impact of present-day border infrastructure on jaguar movement, I found that there are currently several wide potential movement corridors (Figure 2.2b): south of Coronado National Forest and east of Nogales, Mexico and the region due east of Douglas, USA, and Agua Prieta, Mexico (see Figure 2.1 for reference).

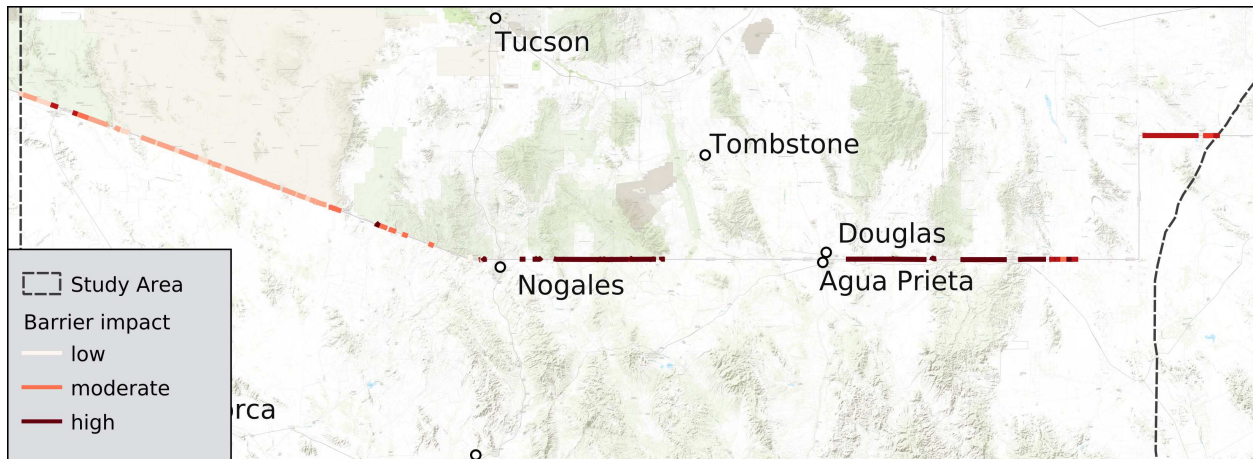


**Figure 2.5:** A map of vehicle barricade segments symbolized based on the amount of current passing through them in the present-day border scenario. Segments with more current passing through them indicate that conversion to pedestrian fencing would have a larger impact on habitat connectivity.

## 2.4 Discussion

My study provides a novel analysis of the effects of U.S.-Mexico border infrastructure on jaguar habitat connectivity. I identified important present-day movement corridors for jaguars. Under likely future scenarios, I expect that the movement corridors that exist today will experience significant impacts from a border infrastructure expansion, and potential trans-border movement will likely become restricted to narrow passages. I also identified sections along the border where conversion from vehicle barriers to pedestrian fencing would have the greatest negative impact on jaguar habitat connectivity.

In addition to inference specific to jaguar connectivity, I developed new methods for incorporating roads into connectivity analyses that can be used to guide future research. The methods I applied provide an improved approach over simpler efforts that use constant resistance values because it accounts for both the footprint *and* the use intensity of a road when assigning a resistance value.

I found that present-day U.S. border infrastructure likely isolates breeding jaguar populations in northern Mexico from habitat in the United States, and that potential border infrastructure expansion threatens further isolation. Present-day border infrastructure clearly reduces the probability of jaguar movement through otherwise-suitable movement pathways. Nearly 100 km of pedestrian

fencing south of Tombstone, Arizona in the U.S. bisects an otherwise probable movement corridor, preventing dispersal through this region. The section of border fencing north of Nogales, Mexico has a similar effect. This may result in a reduced probability of jaguars successfully dispersing into the United States due to the decrease in movement path redundancy. There is also evidence that impacts of present-day infrastructure extend well beyond the border itself (Figure 2.3a), revealing the far-reaching consequences of these barriers.

Despite these impacts, trans-border jaguar dispersal has been documented several times. Even though present-day infrastructure likely reduces the probability of such dispersal events, it does not preclude them. Results show that border infrastructure expansion projects being pursued by the United States government (as of the writing of this thesis) will make these already rare dispersal events even rarer. The expansion considered in this study would result in the interruption and redirection of  $> 50\%$  of the current flow (jaguar movement) predicted to occur in present-day conditions. Present-day movement corridors would become restricted almost entirely to pinch points (Figure 2.2c) (*sensu* McRae et al. 2008), which are narrow areas of high relative probability of movement where the addition of new barriers is likely to result in a disproportionate loss of connectivity (McRae et al. 2008, McClure et al. 2017).

Border infrastructure today results in a decreased probability of movement through suitable habitat throughout the Coronado National Forest that currently provides a primary linkage between habitat in southern Arizona and New Mexico to more northern habitat in the study area – an area predicted to contain extensive high-quality habitat (see Chapter one). Particularly of note is the reduced movement probability in the Coronado National Forest north of Douglas, Arizona. This area is currently home to the only documented jaguar in the United States (Center for Biological Diversity 2017). Results suggest that the conversion from vehicle barriers to pedestrian fencing east of Douglas, AZ will reduce the probability that additional jaguars will be able to access the habitat in this area.

Current flow maps produced by Circuitscape should be interpreted carefully. Low current flow through a given region does not necessarily mean that the region is not an important contributor to

connectivity or that it is not high quality movement habitat. Rather, it may have low current flow because there are many nearby alternative paths from node A to node B (path redundancy) that an animal is equally likely to take. Similarly, high current flow in a given area does not necessarily mean that the area has minimal movement costs. The region may have high current flow because, though highly resistant to movement, it has lower resistance than alternative nearby paths. For an in depth discussion of the circuit theory behind Circuitscape and how to interpret outputs, see McRae et al. (2008).

Establishing and/or identifying trans-border movement corridors for jaguars is listed as a priority in the United States Fish and Wildlife Draft Recovery plan for jaguars (US Fish and Wildlife Service 2016). Conserving and restoring trans-border habitat connectivity gives the northern jaguar population access to habitat in the United States. Expanding the distribution of the northern jaguar meta-population into the United States may have significant conservation benefits, including decreased extinction risk and increased probability that the meta-population as a whole will be resistant or resilient to climate change. In this study I identified areas important for trans-border connectivity, as well as areas where connectivity is most threatened by border wall expansion and conversion to pedestrian fencing (see Figure 2.5). These results could be useful for trans-border connectivity conservation planning.

# Bibliography

- Anantharaman, R., K. Hall, V. Shah, and A. Edelman. 2019. Circuitscape in julia: High performance connectivity modelling to support conservation decisions. arXiv preprint arXiv:1906.03542.
- Bååth, R. 2014. Bayesian first aid: A package that implements bayesian alternatives to the classical \*.test functions in r. UseR! 2014 - the International R User Conference.
- Barbet-Massin, M., F. Jiguet, C. H. Albert, and W. Thuiller. 2012. Selecting pseudo-absences for species distribution models: how, where and how many? *Methods in ecology and evolution*, **3**:327–338.
- Bezanson, J., A. Edelman, S. Karpinski, and V. B. Shah. 2017. Julia: A fresh approach to numerical computing. *SIAM review*, **59**:65–98.
- Bonham-Carter, G. F. 2014. Geographic information systems for geoscientists: modelling with GIS, volume 13. Elsevier.
- Boyce, M. S., P. R. Vernier, S. E. Nielsen, and F. K. Schmiegelow. 2002. Evaluating resource selection functions. *Ecological modelling*, **157**:281–300.
- Boydston, E. E. and C. A. L. González. 2005. Sexual differentiation in the distribution potential of northern jaguars (*Panthera onca*). Pages 51–56 in G. J. Gottfried, B. S. Gebow, L. G. Eskew, and C. B. Edminster, editors. Connecting mountain islands and desert seas: biodiversity and management of the Madrean Archipelago II. USDA Forest Service Proceedings RMRS-P-36.
- Brown, D. E. and C. A. López-González. 2000. Notes on the occurrences of jaguars in arizona and new mexico. *The Southwestern Naturalist*, Pages 537–542.
- Cavalcanti, S. M. C. 2008. Predator-prey relationships and spatial ecology of jaguars in the southern pantanal, brazil: Implications for conservation and management. All Graduate Theses and Dissertations, 112.

- Celeux, G., F. Forbes, C. P. Robert, D. M. Titterington, et al. 2006. Deviance information criteria for missing data models. *Bayesian analysis*, **1**:651–673.
- Center for Biological Diversity. 2017. New video shows wild jaguar in arizona. Press Release. [https://www.biologicaldiversity.org/news/press\\\_releases/2017/jaguar-09-14-2017.php](https://www.biologicaldiversity.org/news/press\_releases/2017/jaguar-09-14-2017.php).
- Center for Biological Diversity. 2019. Trump administration waives laws to build 100 miles of border wall across arizona national monument, wildlife refuges. Press Release. <https://biologicaldiversity.org/w/news/press-releases/trump-administration-waives-laws-to-build-100-miles-border-wall-across-arizona-national-monument-and-refuges-2019-05-14/>.
- Center for International Earth Science Information Network - CIESIN - Columbia University. 2016. Palisades, NY: NASA Socioeconomic Data and Applications Center (SEDAC).
- Crawshaw Jr, P., J. Mahler, C. Indrusiak, S. Cavalcanti, M. Leite-Pitman, and K. Silvius. 2004. Ecology and conservation of the jaguar (*panthera onca*) in iguaçu national park, brazil.
- Crooks, K. R., C. L. Burdett, D. M. Theobald, C. Rondinini, and L. Boitani. 2011. Global patterns of fragmentation and connectivity of mammalian carnivore habitat. *Philosophical Transactions of the Royal Society B: Biological Sciences*, **366**:2642–2651.
- Crooks, K. R. and M. Sanjayan. 2006. *Connectivity conservation*, volume 14. Cambridge University Press.
- Dallimer, M. and N. Strange. 2015. Why socio-political borders and boundaries matter in conservation. *Trends in Ecology & Evolution*, **30**:132–139.
- de la Torre, J. A., J. F. González-Maya, H. Zarza, G. Ceballos, and R. A. Medellín. 2018. The jaguar's spots are darker than they appear: assessing the global conservation status of the jaguar *Panthera onca*. *Oryx*, **52**:300–315.
- de la Torre, J. A., J. M. Núñez, and R. A. Medellín. 2017. Spatial requirements of jaguars and pumas in southern mexico. *Mammalian Biology*, **84**:52–60.

- de la Torre, J. A. and M. Rivero. 2019. Insights of the movements of the jaguar in the tropical forests of southern Mexico. Pages 217–241 in R. Reyna-Hurtado and C. A. Chapman, editors. *Movement Ecology of Neotropical Forest Mammals*. Springer.
- Dickson, B. G., C. M. Albano, B. H. McRae, J. J. Anderson, D. M. Theobald, L. J. Zachmann, T. D. Sisk, and M. P. Dombek. 2017. Informing strategic efforts to expand and connect protected areas using a model of ecological flow, with application to the western United States. *Conservation Letters*, **10**:564–571.
- Dorazio, R. M. 2014. Accounting for imperfect detection and survey bias in statistical analysis of presence-only data. *Global Ecology and Biogeography*, **23**:1472–1484.
- Drusch, M., U. Del Bello, S. Carlier, O. Colin, V. Fernandez, F. Gascon, B. Hoersch, C. Isola, P. Laberinti, P. Martimort, et al. 2012. Sentinel-2: ESA's optical high-resolution mission for global operational services. *Remote Sensing of Environment*, **120**:25–36.
- Echemendia, J. 2009. Waiving environmental concerns along the border: fence construction and the waiver authority of the Real ID Act. *Pitt. J. Environ. Pub. Health L.*, **3**:81.
- Environmental Research Systems, Inc. (ESRI). 2014. *ArcMap 10.3*. Environmental Research Systems, Inc., Redlands, California, USA.
- Fletcher, R. J., R. A. McCleery, D. U. Greene, and C. A. Tye. 2016. Integrated models that unite local and regional data reveal larger-scale environmental relationships and improve predictions of species distributions. *Landscape Ecology*, **31**:1369–1382.
- Forman, R. T., D. Sperling, J. A. Bissonette, A. P. Clevenger, C. D. Cutshall, V. H. Dale, L. Fahrig, R. L. France, K. Heanue, C. R. Goldman, et al. 2003. *Road ecology: science and solutions*. Island Press.
- Foster, R. J., B. J. Harmsen, and C. P. Doncaster. 2010. Habitat use by sympatric jaguars and pumas across a gradient of human disturbance in Belize. *Biotropica*, **42**:724–731.

- Frankham, R. 1998. Inbreeding and extinction: island populations. *Conservation biology*, **12**:665–675.
- Gelman, A., D. B. Rubin, et al. 1992. Inference from iterative simulation using multiple sequences. *Statistical science*, **7**:457–472.
- Giraud, C., C. Calenge, C. Coron, and R. Julliard. 2016. Capitalizing on opportunistic data for monitoring relative abundances of species. *Biometrics*, **72**:649–658.
- Gorelick, N., M. Hancher, M. Dixon, S. Ilyushchenko, D. Thau, and R. Moore. 2017. Google earth engine: Planetary-scale geospatial analysis for everyone. *Remote Sensing of Environment*. URL <https://doi.org/10.1016/j.rse.2017.06.031>.
- Grigione, M. M., K. Menke, C. López-González, R. List, A. Banda, J. Carrera, R. Carrera, A. J. Giordano, J. Morrison, M. Sternberg, R. Thomas, and B. Van Pelt. 2009. Identifying potential conservation areas for felids in the usa and mexico: integrating reliable knowledge across an international border. *Oryx*, **43**:78–86.
- Gutiérrez-González, C. E. and C. A. López-González. 2017. Jaguar interactions with pumas and prey at the northern edge of jaguars' range. *PeerJ*, **5**:e2886.
- Haag, T., A. S. Santos, D. A. Sana, R. G. Morato, L. Cullen Jr, P. G. Crawshaw Jr, C. De Angelo, M. Di Bitetti, F. Salzano, and E. Eizirik. 2010. The effect of habitat fragmentation on the genetic structure of a top predator: loss of diversity and high differentiation among remnant populations of atlantic forest jaguars (*panthera onca*). *Molecular Ecology*, **19**:4906–4921.
- Hanks, E. M., M. B. Hooten, and F. A. Baker. 2011. Reconciling multiple data sources to improve accuracy of large-scale prediction of forest disease incidence. *Ecological Applications*, **21**:1173–1188.
- Hatten, J. R., A. Averill-Murray, and W. E. Van Pelt. 2005. A spatial model of potential jaguar habitat in Arizona. *The Journal of Wildlife Management*, **69**:1024–1033.

- Herbener, K. W., S. J. Tavener, and N. T. Hobbs. 2012. The distinct effects of habitat fragmentation on population size. *Theoretical ecology*, **5**:73–82.
- Hobbs, N. T. and M. B. Hooten. 2015. *Bayesian models: a statistical primer for ecologists*. Princeton University Press.
- Hock, R. J. 1955. Southwestern exotic felids. *American Midland Naturalist*, Pages 324–328.
- Illian, J. B., S. Martino, S. H. Sørbye, J. B. Gallego-Fernández, M. Zunzunegui, M. P. Esquivias, and J. M. J. Travis. 2013. Fitting complex ecological point process models with integrated nested laplace approximation. *Methods in Ecology and Evolution*, **4**:305–315.
- Johnson, D. H. 1980. The comparison of usage and availability measurements for evaluating resource preference. *Ecology*, **61**:65–71.
- Keller, I. and C. R. Largiader. 2003. Recent habitat fragmentation caused by major roads leads to reduction of gene flow and loss of genetic variability in ground beetles. *Proceedings of the Royal Society of London. Series B: Biological Sciences*, **270**:417–423.
- Kennedy, C. M., J. R. Oakleaf, D. M. Theobald, S. Baruch-Mordo, and J. Kiesecker. 2019. Managing the middle: A shift in conservation priorities based on the global human modification gradient. *Global change biology*, **25**:811–826.
- Koshkina, V., Y. Wang, A. Gordon, R. M. Dorazio, M. White, and L. Stone. 2017. Integrated species distribution models: combining presence-background data and site-occupancy data with imperfect detection. *Methods in Ecology and Evolution*, **8**:420–430.
- Lasky, J. R., W. Jetz, and T. H. Keitt. 2011. Conservation biogeography of the us–mexico border: a transcontinental risk assessment of barriers to animal dispersal. *Diversity and Distributions*, **17**:673–687.

- Linnell, J. D., A. Trouwborst, L. Boitani, P. Kaczensky, D. Huber, S. Reljic, J. Kusak, A. Majic, T. Skrbinek, H. Potocnik, et al. 2016. Border security fencing and wildlife: the end of the transboundary paradigm in eurasia? *PLoS biology*, **14**:e1002483.
- List, R. 2007. The impacts of the border fence on wild mammals. *A Barrier to our Shared Environment: The Border Wall between Mexico and the United States*, Pages 77–86.
- MacKenzie, D. I., J. D. Nichols, G. B. Lachman, S. Droege, J. Andrew Royle, and C. A. Langtimm. 2002. Estimating site occupancy rates when detection probabilities are less than one. *Ecology*, **83**:2248–2255.
- Manly, B., L. McDonald, D. L. Thomas, T. L. McDonald, and W. P. Erickson. 2007. *Resource selection by animals: statistical design and analysis for field studies*. Springer Science & Business Media.
- McCain, E. B. and J. L. Childs. 2008. Evidence of resident jaguars (*panthera onca*) in the southwestern united states and the implications for conservation. *Journal of Mammalogy*, **89**:1–10.
- McClure, M. L., B. G. Dickson, and K. L. Nicholson. 2017. Modeling connectivity to identify current and future anthropogenic barriers to movement of large carnivores: A case study in the American Southwest. *Ecology and Evolution*, **7**:3762–3772.
- McRae, B. H., B. G. Dickson, T. H. Keitt, and V. B. Shah. 2008. Using circuit theory to model connectivity in ecology, evolution, and conservation. *Ecology*, **89**:2712–2724.
- McRae, B. H. and V. B. Shah. 2009. *Circuitscape user’s guide*. The University of California, Santa Barbara.
- Menke, K. A. and C. L. Hayes. 2003. Evaluation of the relative suitability of potential jaguar habitat in New Mexico. Technical report, New Mexico Department of Game and Fish, Albuquerque, New Mexico.

- Morato, R. G., J. J. Thompson, A. Paviolo, J. A. de La Torre, F. Lima, R. T. McBride Jr., R. C. Paula, et al. 2018. Jaguar movement database: a gps-based movement dataset of an apex predator in the neotropics. *Ecology*, **99**:1691.
- Norman, L., H. Huth, L. Levick, I. Shea Burns, D. Phillip Guertin, F. Lara-Valencia, and D. Semmens. 2010. Flood hazard awareness and hydrologic modelling at ambos nogales, united states–mexico border. *Journal of Flood Risk Management*, **3**:151–165.
- Northrup, J. M., M. B. Hooten, C. R. Anderson, and G. Wittemyer. 2013. Practical guidance on characterizing availability in resource selection functions under a use–availability design. *Ecology*, **94**:1456–1463.
- Noss, R. F., H. B. Quigley, M. G. Hornocker, T. Merrill, and P. C. Paquet. 1996. Conservation biology and carnivore conservation in the rocky mountains. *Conservation Biology*, **10**:949–963.
- Nuñez-Perez, R. and B. Miller. 2019. Movements and home range of jaguars (*panthera onca*) and mountain lions (*puma concolor*) in a tropical dry forest of western mexico. Pages 243–262 *in* Movement Ecology of Neotropical Forest Mammals. Springer.
- Opdam, P. and D. Wascher. 2004. Climate change meets habitat fragmentation: linking landscape and biogeographical scale levels in research and conservation. *Biological conservation*, **117**:285–297.
- OpenStreetMap contributors. 2017. Planet dump retrieved from <https://planet.osm.org>. Data downloaded from <https://download.geofabrik.de/>.
- Patrick-Birdwell, C., S. Avila-Villegas, J. Neeley, and L. Misztal. 2013. Mapping and assessing the environmental impacts of border tactical infrastructure in the sky island region. Pages 365–369 *in* G. J. Gottfried, P. F. Ffolliott, B. S. Gebow, L. G. Eskew, and L. C. Collins, editors. Merging science and management in a rapidly changing world: Biodiversity and management of the Madrean Archipelago III; 2012 May 1-5; Tucson, AZ. Proceedings. RMRS-P-67. Fort Collins, CO: U.S. Department of Agriculture, Forest Service, Rocky Mountain Research Station.

- Peters, R., W. J. Ripple, C. Wolf, M. Moskwik, G. Carreón-Arroyo, G. Ceballos, A. Córdova, R. Dirzo, P. R. Ehrlich, A. D. Flesch, et al. 2018. Nature divided, scientists united: US–Mexico border wall threatens biodiversity and binational conservation. *BioScience*, **68**:740–743.
- Piekielek, J. 2009. Public Wildlands at the US-Mexico border: where conservation, migration, and border enforcement collide.
- Pinheiro, J., D. Bates, S. DebRoy, D. Sarkar, and R Core Team. 2018. nlme: Linear and Nonlinear Mixed Effects Models. URL <https://CRAN.R-project.org/package=nlme>. R package version 3.1-137.
- Pokorny, B., K. Flajšman, L. Centore, F. S. Krope, and N. Šprem. 2017. Border fence: a new ecological obstacle for wildlife in southeast europe. *European journal of wildlife research*, **63**:1.
- R Core Team. 2019. R: A Language and Environment for Statistical Computing. R Foundation for Statistical Computing, Vienna, Austria. URL <http://www.R-project.org/>.
- Reveal from The Center for Investigative Reporting and OpenStreetMap contributors. 2017. GIS data for the U.S.-Mexico border fence. [https://github.com/cirlabs/border\\_fence\\_map](https://github.com/cirlabs/border_fence_map).
- Ribeiro Jr., P. J. and P. J. Diggle. 2018. geoR: Analysis of Geostatistical Data. URL <https://CRAN.R-project.org/package=geoR>. R package version 1.7-5.2.1.
- Rosas-Rosas, O. C., L. C. Bender, and R. Valdez. 2010. Habitat correlates of jaguar kill-sites of cattle in northeastern sonora, mexico. *Human-Wildlife Interactions*, **4**:103–111.
- Rouse, J. W., R. H. Haas, J. A. Schell, and D. W. Deering. 1974. Monitoring vegetation systems in the Great Plains with ERTS. *Proceedings of the third Earth Resources Technology Satellite Symposium, NASA SP-351*, Pages 309–317.
- Rozyłowicz, L., V. D. Popescu, M. Pătroescu, and G. Chișamera. 2011. The potential of large carnivores as conservation surrogates in the romanian carpathians. *Biodiversity and Conservation*, **20**:561–579.

- Ruiz-Gutiérrez, V., T. A. Gavin, and A. A. Dhondt. 2008. Habitat fragmentation lowers survival of a tropical forest bird. *Ecological Applications*, **18**:838–846.
- Sanderson, E. W. and K. Fisher. 2011. Digital mapping in support of recovery planning for the northern jaguar. Final report under agreement F11AC00036 (and modification #0001) between the US Fish and Wildlife Service and the Wildlife Conservation Society, Pages 1–11.
- Sanderson, E. W., K. H. Redford, C. B. Chetkiewicz, R. A. Medellin, A. R. Rabinowitz, J. G. Robinson, and A. B. Taber. 2002. Planning to save a species: the jaguar as a model. *Conservation Biology*, **16**:58–72.
- Secretaría de Medio Ambiente y Recursos Naturales. 2010. Oficial Mexicana NOM-059-SEMARNAT-2010, protección ambiental-especies nativas de México de flora y fauna silvestres-categorías de riesgo y especificaciones para su inclusión, exclusión o cambio-lista de especies en riesgo. Secretaría de Medio Ambiente y Recursos Naturales, Diario Oficial.
- Serrat-Capdevila, A., J. B. Valdés, J. G. Pérez, K. Baird, L. J. Mata, and T. Maddock III. 2007. Modeling climate change impacts—and uncertainty—on the hydrology of a riparian system: The San Pedro Basin (Arizona/Sonora). *Journal of Hydrology*, **347**:48–66.
- Setton, E., P. Hystad, and P. Keller. 2005. Road classification schemes - good indicators of traffic volume? University of Victoria Spatial Sciences Laboratories Working Paper, Pages 05–014.
- Seymour, K. L. 1989. *Panthera onca*. *Mammalian species*, Pages 1–9.
- Sky Island Alliance. 2019. Madrean archipelago biodiversity assessment. <http://madrean.org/symbfauna/>. Accessed: 2018-05-24.
- Sollmann, R., M. M. Furtado, H. Hofer, A. T. Jacomo, N. M. Torres, and L. Silveira. 2012. Using occupancy models to investigate space partitioning between two sympatric large predators, the jaguar and puma in central Brazil. *Mammalian Biology-Zeitschrift für Säugetierkunde*, **77**:41–46.

- Spearman, C. 1904. The proof and measurement of association between two things. *American journal of Psychology*, **15**:72–101.
- Spiegelhalter, D. J., N. G. Best, B. P. Carlin, and A. Van Der Linde. 2002. Bayesian measures of model complexity and fit. *Journal of the Royal Statistical Society: Series B (Statistical Methodology)*, **64**:583–639.
- Tadono, T., H. Ishida, F. Oda, S. Naito, K. Minakawa, and H. Iwamoto. 2014. Precise global dem generation by alos prism. *ISPRS Annals of the Photogrammetry, Remote Sensing and Spatial Information Sciences*, **2**:71.
- Theobald, D. M. 2008. Network and accessibility methods to estimate the human use of ecosystems. *in* Proceedings of the 11th AGILE international conference on geographic information science. University of Girona, Spain.
- Theobald, D. M. 2010. Estimating natural landscape changes from 1992 to 2030 in the conterminous US. *Landscape Ecology*, **25**:999–1011.
- Theobald, D. M. 2013. A general model to quantify ecological integrity for landscape assessments and US application. *Landscape Ecology*, **28**:1859–1874.
- Theobald, D. M. 2016. A general-purpose spatial survey design for collaborative science and monitoring of global environmental change: The global grid. *Remote Sensing*, **8**:813.
- Theobald, D. M., D. Harrison-Atlas, W. B. Monahan, and C. M. Albano. 2015. Ecologically-relevant maps of landforms and physiographic diversity for climate adaptation planning. *PloS one*, **10**:e0143619.
- Thornton, D., K. Zeller, C. Rondinini, L. Boitani, K. Crooks, C. Burdett, A. Rabinowitz, and H. Quigley. 2016. Assessing the umbrella value of a range-wide conservation network for jaguars (*panthera onca*). *Ecological Applications*, **26**:1112–1124.

- Tilman, D., R. M. May, C. L. Lehman, and M. A. Nowak. 1994. Habitat destruction and the extinction debt. *Nature*, **371**:65.
- Trouwborst, A., F. Fleurke, and J. Dubrulle. 2016. Border fences and their impacts on large carnivores, large herbivores and biodiversity: An international wildlife law perspective. *Review of European, Comparative & International Environmental Law*, **25**:291–306.
- US Fish and Wildlife Service. 1997. Endangered and threatened wildlife and plants; final rule to extend endangered status for the jaguar in the united states. *Federal Register*, **62**:39147–39157.
- US Fish and Wildlife Service. 2013. Endangered and threatened wildlife and plants; designation of critical habitat for jaguar: Proposed rule. Revised, **78**:39237–39250.
- US Fish and Wildlife Service. 2016. Jaguar Draft Recovery Plan.
- Valdez, R., O. C. R. Rosas, and R. N. Pérez. 2019. Jaguar and puma in mexico. *Wildlife Ecology and Management in Mexico*, 222.
- Vellend, M., K. Verheyen, H. Jacquemyn, A. Kolb, H. Van Calster, G. Peterken, and M. Hermy. 2006. Extinction debt of forest plants persists for more than a century following habitat fragmentation. *Ecology*, **87**:542–548.
- Wang, P., C. Huang, E. C. Brown de Colstoun, J. C. Tilton, and B. Tan. 2017. Global Human Built-up and Settlement Extent (HBASE) Dataset from LANDSAT. NASA Socioeconomic Data and Applications Center (SEDAC), Palisades, NY, USA.
- Ward, G., T. Hastie, S. Barry, J. Elith, and J. R. Leathwick. 2009. Presence-only data and the EM algorithm. *Biometrics*, **65**:554–563.
- Wildlife Conservation Society. 2015. Jaguar observations database. <https://jaguardata.info>. Accessed: 2017-03-10.

- Williams, P. J., M. B. Hooten, J. N. Womble, G. G. Esslinger, M. R. Bower, and T. J. Hefley. 2017. An integrated data model to estimate spatiotemporal occupancy, abundance, and colonization dynamics. *Ecology*, **98**:328–336.
- Wooldridge, R. L., R. J. Foster, and B. J. Harmsen. 2019. The functional role of scent marking in the social organization of large sympatric neotropical felids. *Journal of Mammalogy*, **100**:445–453.
- Zazueta-Castro, L. 2019. Nearly 30 laws waived in starr county for wall construction. *The Monitor*. URL <https://www.themonitor.com/2019/06/30/nearly-30-laws-waived-starr-county-wall-construction/>.
- Zeller, K. A., M. K. Jennings, T. W. Vickers, H. B. Ernest, S. A. Cushman, and W. M. Boyce. 2018. Are all data types and connectivity models created equal? validating common connectivity approaches with dispersal data. *Diversity and distributions*, **24**:868–879.
- Ziegler, A. D., T. W. Giambelluca, D. Plondke, S. Leisz, L. T. Tran, J. Fox, M. A. Nullet, J. B. Vogler, D. M. Troung, and T. D. Vien. 2007. Hydrological consequences of landscape fragmentation in mountainous northern vietnam: buffering of hortonian overland flow. *Journal of Hydrology*, **337**:52–67.

# Appendix A

## A.1 JaguarData.info Selection Criteria

The criteria below were used to select the jaguar observations included in this download from the database. Data were downloaded on March 10th, 2017.

**Years:** From 1985 to 2012

**States:** all (except unknown)

**Location types:** Defined Point, Determined Point

**Observation types:** Bounty paid, Capture event, Dead specimen, Hunting event, Killed after depredation, Live sighting, Other mortality, Photograph seen, Predation event, Scientific study, Sign seen, Structured interviews

**Evidence types:** Carcass measured, DNA, First hand report, Hide, Live jaguar capture, Photograph or video, Plaster cast of tracks, Prey animal killed jaguar style, Scat or hair collected, Second hand report, Skull and/or bones, Telemetry data, Tracks seen and/or measured

**Date types:** Exact Date, Month-Year, Season within a Year, Year, Few Years, Prior to a given year

**Identity types:** Jaguar

**Sex types:** Female - certain, Female - uncertain, Male - certain, Male - uncertain, Unknown or unattributed

## A.2 Bayesian Directed Acyclic Graph

Below is a directed acyclic graph (DAG) representation of the integrated species distribution model used in Chapter one. Parameter names match those used in section 1.2.3.

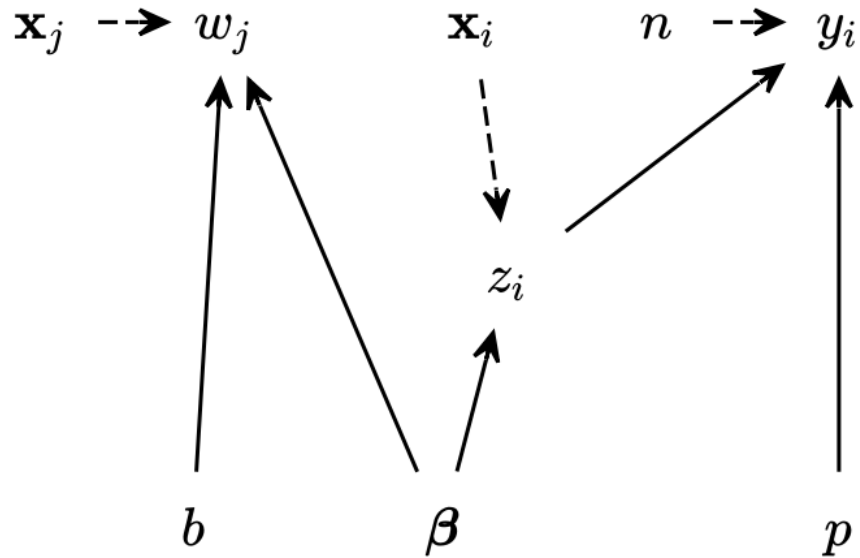


**Figure A.1:** A Directed acyclic graph representation of the integrated species distribution model developed for Chapter one.

### A.3 Riparian Vegetation and Water Classification

Riparian vegetation and water were both independently classified as binary images using a random forest supervised classification algorithm in Google Earth Engine (Gorelick et al. 2017). The classification process used in this study can be broken down into three primary steps: training data collection, image classification, and validation.

#### A.3.1 Training Data Collection

I used a spatially balanced opportunistic sampling design to generate training data in Google Earth Engine. To distribute sampling effort evenly and randomly throughout the study area, I generated a random sample ( $n = 80$ ) of level 9 chips ( $0.35156 \times 0.35156$  decimal degree rectangles) from the Global Grid (Theobald 2016) and digitized points opportunistically in each chip. For the purposes of this study, riparian vegetation is defined as woody or herbaceous vegetation within the valley bottom that is influenced by the presence of water and is typically not found in areas upland of the valley bottom. I digitized 2,486 training points for riparian vegetation classification and

1,876 training points for water classification. Additional training points were recursively added to the training dataset over the course of several preliminary image classifications to correct false negatives and false positives for both riparian and water classification. A total of 486 training points were added for riparian vegetation classification and 431 training points were added for water classification.

### **A.3.2 Image Classification**

I used a random forest classification algorithm in Google Earth Engine for classifying water and riparian vegetation. Binary classifications of water and riparian vegetation were generated separately and independently. The bands and the calculations used to derive them are described below. Sentinel-derived bands were generated using Sentinel 2 imagery (Drusch et al. 2012), and Elevation-derived bands were generated using the ALOS world 3D 30 meter digital surface model (Tadono et al. 2014).

#### **Riparian Vegetation**

An multi-band image with bands described below was classified to predict riparian vegetation.

##### **Sentinel-derived Bands**

- Median value for all Sentinel bands between March 1st and July 31st in 2016 and 2017.
- Median NDVI value between March 1st and July 31st in 2016 and 2017.
- Coefficient of variation of NDVI over time, derived from Sentinel images falling between January 1st and December 31st in 2016 and 2017.
- Deviation of NDVI (using median NDVI described above) from its neighborhood mean, calculated for three neighborhood radii: 270, 540, and 810 meters.

##### **Elevation-derived Bands**

- Raw elevation

- Slope
- Continuous Heat Insolation Load Index (CHILI; Theobald et al. 2015) derived using ALOS DEM at 30 meters.
- Deviation of elevation from the neighborhood mean of elevation. Calculated for three neighborhood radii: 180, 270, and 540 meters.
- Elevation z-score relative to neighborhood mean. Calculated as the elevation value minus the neighborhood mean (calculated as above) divided by the neighborhood standard deviation. Calculated for three neighborhood radii: 180, 270, and 540 meters.

## **Water**

An multi-band image with bands described below was classified to predict surface water.

### **Sentinel-derived bands**

- Median value for all Sentinel bands between March 1st and July 31st in 2016 and 2017.

### **Elevation-derived Bands**

- Slope
- Deviation of elevation from the neighborhood mean of elevation. Calculated for three neighborhood radii: 180, 270, and 540 meters.

## **A.3.3 Post Processing of Riparian Vegetation**

In an effort to improve classification accuracy and remove small patches of riparian vegetation in the classified image, riparian patches of 4 pixels or less were removed from the classified image. Validation was performed on this image rather than the raw classification.

## **A.3.4 Validation**

Classified images of riparian vegetation and water were each validated using the following methods. First, validation points were generated using a stratified random sample of the classified

images. Three sampling strata were defined: 1) Pixels classified as 1, (2) pixels classified as 0 and within 100 meters of a pixel classified as 1, and (3) pixels classified as 0 and at least 100 meters away from the nearest pixel classified as one. I split pixels classified as 0 into two separate strata (strata 2 and 3) because I hypothesized that the rate of false negatives may vary depending on proximity to the nearest classified 1. Specifically, I expected a higher false negative rate in regions (stratum 2) closer to classified 1s.

180 points were randomly sampled within each stratum for both water and riparian vegetation, resulting in a total of 540 validation points for each classification. The true value of each validation point was recorded using heads-up digitizing of color composite Sentinel imagery (and Google Satellite imagery in cases where the true class could not be determined from Sentinel imagery alone). The predicted class was recorded for each point in addition to the true value to create a confusion matrix for water and riparian vegetation classifications. Table A.1 and Table A.2 show classification accuracy by stratum.

**Table A.1:** Confusion matrix by validation stratum for riparian vegetation classification.

		<b>Counts</b>		
<b>Predicted value</b>		Stratum 1	Stratum 2	Stratum 3
	0	180	164	27
	1	0	16	153
	Accuracy	100%	91.1%	85.0%

**Table A.2:** Confusion matrix by validation stratum for water classification.

<b>Counts</b>			
<b>Predicted value</b>	Stratum 1	Stratum 2	Stratum 3
0	180	161	7
1	0	19	173
Accuracy	100%	89.4%	96.1%

## A.4 Integrated Likelihood

I used the following integrated likelihood to calculate DIC for model selection, arrived at by integrating  $z$  out from the joint likelihood in eq. 1.8.

$$\begin{aligned}
 [\mathbf{y}, \mathbf{w} | b, p, \boldsymbol{\beta}] &= \prod_{i=1}^{288} \left[ 1 - \psi_i \left( 1 - \binom{J_i}{y_i} (p)^{y_i} (1-p)^{J_i - y_i} \right) \right] \times \\
 &\quad \prod_{j=1}^{25056} \left[ (b\psi_j)^{w_j} (1 - b\psi_j)^{1-w_j} \right] \tag{A.1} \\
 \psi_j &= \text{logit}^{-1}(\mathbf{x}'_j \boldsymbol{\beta}) \\
 \psi_i &= \text{logit}^{-1}(\mathbf{x}'_i \boldsymbol{\beta})
 \end{aligned}$$

## A.5 Variogram

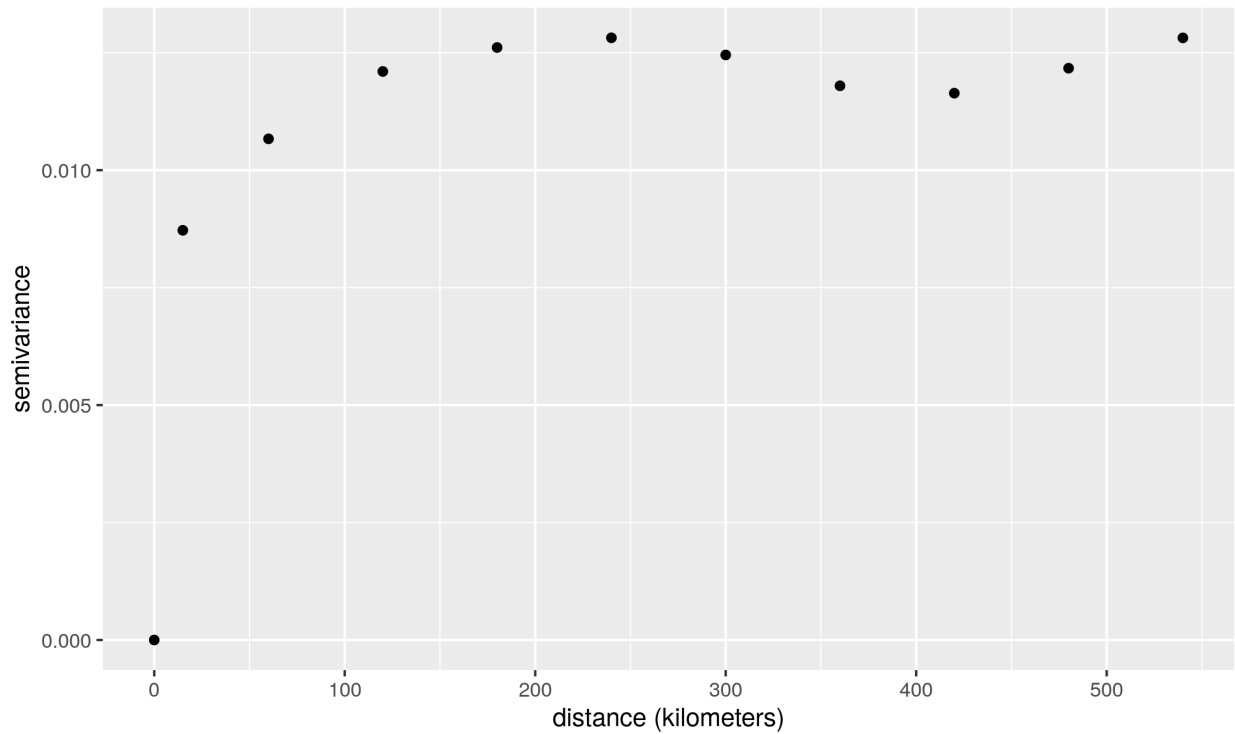


**Figure A.2:** A variogram for the residuals (observed - predicted) of model predictions for the presence/background locations used for model fitting. Generated using the `variog()` function in the `geoR` package for R (Ribeiro Jr. and Diggle 2018)

# Appendix B

**Table B.1:** Summary of resistance surface inputs. Note that layers were rescaled when combined for the final resistance surfaces.

Input Layer	Layer Source	Resistance Description	Scale (resolution)	Resistance	Range
Habitat Suitability (HS)	Chapter one	The complement of the rescaled habitat suitability map.	30 meters	$R_{HS} = \left(1 - \frac{HS}{\max(HS)}\right)$	0 - 1
Human Modification (HM)	Calculated following Kennedy et al. (2019)	Human modification (sensu Theobald 2013)	300 meters	$R_{HM} = HM$	0 - 1
Roads	OpenStreetMap contributors (2017)	Resistance of roads defined using mean estimated traffic ( $t$ ) for each road type adjusted by accessibility ( $A$ )	1:10000	$R_r = t \times A$	0.00093 - 1
Border infrastructure	Reveal from The Center for Investigative Reporting and OpenStreetMap contributors (2017)	Resistance defined based on the type of border infrastructure: pedestrian fencing (p), or vehicle barriers (v)	NA	$R_b = \begin{cases} \infty & \text{if type = p} \\ 1^* & \text{if type = v} \end{cases}$	1 - $\infty$

\*For the expanded wall scenario,  $R_b = \infty$  for type = v, as these sections were "converted" to pedestrian fencing in the expanded wall scenario.